IEEE Access
Multidisciplinary | Rapid Review | Open Access Journal

Received 18 January 2024, accepted 28 January 2024, date of publication 5 February 2024, date of current version 16 February 2024.

Digital Object Identifier 10.1109/ACCESS.2024.3362337

RESEARCH ARTICLE

Optimal Application of Mobile Substation Resources for Transmission System Restoration Under Flood Events

JOSHUA J. YIP[1], (Member, IEEE), VINICIUS C. CUNHA[2], (Member, IEEE), BRENT G. AUSTGEN[3], (Graduate Student Member, IEEE), SURYA SANTOSO[1], (Fellow, IEEE), ERHAN KUTANOGLU[3], AND JOHN J. HASENBEIN[3]

[1]Chandra Family Department of Electrical and Computer Engineering, The University of Texas at Austin, Austin, TX 78712, USA
[2]Energy Research and Analytics, Campinas, São Paulo 13087-570, Brazil
[3]Operations Research and Industrial Engineering, The University of Texas at Austin, Austin, TX 78712, USA

Corresponding author: Joshua J. Yip (joshua.yip@utexas.edu)

This work was supported in part by the Energy Institute of The University of Texas at Austin through the Fueling a Sustainable Energy Transition research initiative.

ABSTRACT This article studies the Transmission Restoration Problem with Mobile Substation Resources, a novel mixed-integer linear programming model that prescribes the most effective usage of mobile-substation resources to enhance the resilience of a power transmission system against a particular, widespread flood event. The model is a two-stage stochastic program in which each scenario captures a different potential progression of flood heights at substations over the event horizon. The first stage concerns the pre-event selection and positioning of mobile-substation resources. The second stage concerns the coordination of mobile-substation resource deployment and permanent-substation restoration to maintain and recover service within the horizon. Experiments in the IEEE 24-Bus System and a synthetic Houston grid confirm the efficacy of the model. Even when isolated from effects related to restoration of permanent substations, the effect of four mobile transformers and eight mobile breakers for a realistic set of flood scenarios in the synthetic Houston grid was found to be an average total-cost reduction of approximately \$35MM (i.e., approximately 8% of a default optimal objective value). Additionally, a novel, parallel heuristic is designed that can efficiently solve the problem as well as, with minor modifications, similar stochastic problems on pre-selection of mobile resources or placement of static ones. For a 40-scenario model instance in the IEEE 24-Bus System, the extensive form was not able to find an integer-feasible solution in six hours, yet the heuristic achieved an optimality gap no worse than 4.5% in two hours.

INDEX TERMS Floods, power outages, power system restoration, power transmission, resilience, resource management, substations.

NOMENCLATURE

INITIALISMS

MT/MB/MS	Mobile xfmr/breaker/substation.
LT/FT	Limited/full traversability.

SETS

$\mathcal{S}/\mathcal{Z}/\mathcal{N}$	Set of scenarios/depots/substations.
$\mathcal{T}$	Set of time intervals.
$\mathcal{T}^s_{\mathrm{LT}}/\mathcal{T}^s_{\mathrm{FT}}$	Subset of time intervals with LT/FT in scenario s.
$\mathcal{U}/\mathcal{W}$	Set of one-sided/two-sided voltage ratings.
Γ/Ξ	Set of one-sided/two-sided connection sites.
Λ/Λ'	Set of undir./dir. branches.
$\mathcal{L}/\mathcal{L}'$	Set of undir./dir. lines.
$\mathcal{L}_{u,\mathrm{O}}/\mathcal{L}_{u,\mathrm{D}}$	Subset of undir. lines rated u at orig./dest.
$\mathcal{X}/\mathcal{X}'$	Set of undir./dir. branch xfmrs.
$\mathcal{X}_w/\mathcal{X}'_w$	Subset of undir./dir. branch xfmrs rated w.
$\mathcal{I}$	Set of buses.
$\mathcal{I}_{w,\mathrm{G}}/\mathcal{I}_{w,\mathrm{L}}$	Subset of buses rated w for gen./dist.

The associate editor coordinating the review of this manuscript and approving it for publication was Ehab Elsayed Elattar.

FIRST-STAGE PARAMETERS

M/ϵ	Very large/small positive number.
Δt	Duration of time interval [hours].
A_u/A_{TTL}	Allowance of MBs rated u / in total irrespective of rating.
E_w/E_{TTL}	Allowance of MTs rated w / in total irrespective of rating.
K_{zn}	1 if depot z reaches sub. n during LT; o.w. 0.
Ψ_{zw}/Ψ_{zu}	Cost of staging, at depot z, MT rated w / MB rated u [$].
$S_{w,\text{T}}$	Cap. of MT rated w [MVA].
$\ddot{V}_i$	Target voltage mag. at bus i [pu].
$\overline{V}_i/\underline{V}_i$	Voltage mag. limits at bus i [pu].
$\overline{S}_{i,\text{G}}/\overline{S}_{i,\text{L}}$	Original gen./dist. xfmr cap. at bus i [MVA].
$\overline{COS}/\underline{COS}$	Limits for arbitrary value representing cosine of branch angle diff.
$\overline{\delta}$	Maximum absolute value allowed for branch angle diff. [radians].
G_λ/B_λ	Conduct./suscept. of undir. branch λ [pu].
$\overline{S}_\lambda$	Original cap. of undir. branch λ [MVA].
Υ_s	Probability of scenario s.

SECOND-STAGE PARAMETERS

O_n^{st}	1 if sub. n disabled by end of int. t; o.w. 0.
$O_{i,\text{GM}}^{st}$	1 if gen. machine at bus i disabled by end of int. t; o.w. 0.
R_n^{st}	1 if flood height at sub. n above disabling threshold in int. t; o.w. 0.
Ω_n^{st}	1 if sub. n accessible in int. t; o.w. 0.
$\overline{Y}^{st}/\overline{Y}_n^{st}$	Maximum new restoration labor in int. t system-wide / at sub. n [crew-hours].
Ψ_n^s	Total labor required for reinstatement of sub. n [crew-hours].
$\acute{\Psi}_{i,\text{T}}^s/\acute{\Psi}_x^s$	Cost of installing MT at bus i / undir. branch xfmr x [$].
$\acute{\Psi}_{i,\text{B}}^s$	Cost of installing MB at bus i [$].
$\Phi_{i,\text{G}}^{st}/\Phi_{i,\text{L}}^{st}$	Gen. cost per unit energy / value of lost load at bus i in int. t [$/MWh].
$\overline{P}_i^s$	Real gen. cap. at bus i [MW].
$\overline{Q}_i^s/\underline{Q}_i^s$	Reactive gen. limits at bus i [Mvar].
D_i^{st}/F_i^{st}	Real [MW] / reactive [Mvar] load demand at bus i in int. t.

FIRST-STAGE VARIABLES

j_{ST}	Cost of staging MS resources [$].
a_{zu}	Qty. of MBs rated u staged at depot z.
e_{zw}	Qty. of MTs rated w staged at depot z.

SECOND-STAGE VARIABLES

$j_{s,\text{IN}}$	Cost of installing MS resources [$].
$j_{s,\text{G}}/j_{s,\text{L}}$	Cost of real power gen. / load shed [$].
$a_{zl,\text{O}}^{st}/a_{zl,\text{D}}^{st}$	1 if MB dispatched from depot z to orig./dest. of undir. line l in LT int. t; o.w. 0.
$a_{l,\text{O}}^{st}/a_{l,\text{D}}^{st}$	1 if MB deployed at orig./dest. of undir. line l in int. t; o.w. 0.
$\hat{a}_{l,\text{O}}^{st}/\hat{a}_{l,\text{D}}^{st}$	1 if MB oper. at orig./dest. of undir. line l in int. t; o.w. 0.
$\acute{a}_{l,\text{O}}^{st}/\acute{a}_{l,\text{D}}^{st}$	1 if MB newly installed at orig./dest. of undir. line l in int. t; o.w. 0.
e_{zx}^{st}	Qty. of MTs dispatched from depot z to undir. branch xfmr x in LT int. t.
$e_x^{st}/\hat{e}_x^{st}/\acute{e}_x^{st}$	Qty. of MTs deployed / oper. / newly installed at undir. branch xfmr x in int. t.
$e_{zi,\text{G}}^{st}/e_{zi,\text{L}}^{st}$	Qty. of MTs dispatched from depot z to gen./dist. at bus i in LT int. t.
$e_{i,\text{G}}^{st}/e_{i,\text{L}}^{st}$	Qty. of MTs deployed at gen./dist. at bus i in int. t.
$\hat{e}_{i,\text{G}}^{st}/\hat{e}_{i,\text{L}}^{st}$	Qty. of MTs oper. at gen./dist. at bus i in int. t.
$\acute{e}_{i,\text{G}}^{st}/\acute{e}_{i,\text{L}}^{st}$	Qty. of MTs newly installed at gen./dist. at bus i in int. t.
y_n^{st}	New restoration labor at sub. n in int. t [crew-hours].
$\mu_n^{st}/\hat{\mu}_n^{st}$	1 if sub. n reinstated/oper. in int. t; o.w. 0.
h_i^{st}	Real load shed at bus i in int. t [MW].
η_i^{st}	Deviation from target voltage mag. at bus i in int. t [pu].
v_i^{st}/θ_i^{st}	Voltage mag. [pu] / angle [radians] at bus i in int. t.
$p_{i,\text{G}}^{st}/q_{i,\text{G}}^{st}$	Real [MW] / reactive [Mvar] gen. output at bus i in int. t.
d_i^{st}/f_i^{st}	Real [MW] / reactive [Mvar] load supplied at bus i in int. t.
ζ_i^{st}	Load-shed proportion at bus i in int. t.
$\hat{\sigma}_\lambda^{st}$	1 if undir. branch λ oper. in int. t; o.w. 0.
$\sigma_{l,\text{O}}^{st}/\sigma_{l,\text{D}}^{st}$	1 if orig./dest. of undir. line l connected in int. t; o.w. 0.
cos_λ^{st}	Arbitrary value representing cosine of angle diff. of undir. branch λ in int. t.
$\delta_{\lambda'}^{st}$	Voltage angle diff. of dir. branch λ' in int. t [radians].
$p_{\lambda'}^{st}/q_{\lambda'}^{st}$	Real [MW] / reactive [Mvar] power flow within dir. branch λ' in int. t.

OTHER NOTATION

$o(\lambda/\lambda')$	Orig. bus of undir./dir. branch λ/λ'.
$d(\lambda/\lambda')$	Dest. bus of undir./dir. branch λ/λ'.
$n(i/x/\xi/\gamma)$	Sub. containing bus i / undir. branch xfmr x / two-sided connection site ξ / one-sided connection site γ.
$v(\lambda')$	Undir. version of dir. branch λ'.

I. INTRODUCTION

Along coastal areas, hurricanes are common occurrences that cause many utility customers to lose power. When Hurricane Harvey impacted the Gulf Coast of the United States in August 2017, a total of more than 2 million customers in Texas, Louisiana, Mississippi, and Arkansas lost power over the course of roughly two weeks [1]. Much of the loss of service during a hurricane can be attributed to two aspects: high-speed winds that cripple power lines and excessive rain

that debilitates substations. Harvey made landfall with wind speeds exceeding 130 miles per hour, and the stalling of Harvey as it moved inland resulted in 40 to 50 inches of rainfall in some parts of Texas [1].

Indeed, while it is widely known that winds caused substantial damage to the electric grid in past hurricanes and other extreme weather events, the damage caused by flooding also should not be understated. During Hurricane Harvey, the service area of Entergy Texas saw flooding of 17 substations [2], [3], six of which had connected generation capacity totaling 2.285 GW [1], [3]. The service area of CenterPoint Energy in Houston, Texas, saw flooding during Harvey as well; in particular, the flooding of the Memorial substation alone interrupted service to approximately 12,500 customers [4]. Moreover, there have transpired hurricanes with even more severe substation flooding than during Harvey. In 2016, a year before Harvey, Hurricane Matthew flooded as many as 115 substations in North and South Carolina [5]. Likewise, estimates for the number of substations flooded in North Carolina during Hurricane Florence in 2018 have included 64 substations [2] or 55 primary (i.e., transmission) substations [6].

The present article makes two novel contributions:

(I) A stochastic mixed-integer linear programming (MILP) model is developed for application of mobile-substation (MS) resources to enhance the resilience of a transmission system against an imminent, widespread flood event, such as a hurricane. The model considers substations at the transmission level, not the distribution level, because transmission substations are directly connected to one another through lines. The most novel characteristic of the model is its consideration of MS resources.

(II) A parallel heuristic is designed based on the intuitive notion of formations. The heuristic can efficiently solve the problem as well as, with minor modifications, similar stochastic problems on pre-selection of mobile resources or placement of static ones.

A. PRACTICAL CONSIDERATIONS OF SUBSTATION FLOODING

Substation busbars and power lines—even at the distribution level—are generally supported at heights of at least 10 feet [7]. Additionally, substation breakers and transformers usually have their main electrical contacts on top. However, the control cabinets of substation breakers and transformers are commonly no more than a meter above ground [8], [9]. Damage from water ingress to the motors and terminal blocks housed within the cabinets of these components can render the components inoperable [10], [11]. Control houses at substations also contain critical protective relay systems and are susceptible to flood damage [1], [10], [11]. The loss of interconnecting transmission assets such as substations can prevent the delivery of power from generators to loads by inducing the complete absence of a conducting path, the overload of branch capacities, or the violation of bus voltage limits [1], [11].

Throughout Hurricane Harvey, the Electric Reliability Council of Texas coordinated and advised the planning of generator owners, as well as of transmission owners and operators, within the state of Texas for preemptive shutdowns and restorative operations [1]. Besides such actions and extant hardening, the deployment of mobile substations has been credited with the prompt recovery of service after some incidents of substation flooding during Harvey [12], [13], [14]. A mobile substation (MS) is a set of substation components transported on a trailer and thus specially designed to be lightweight and compact [15]. The components of an MS, which typically include a power transformer and one or more breakers along with auxiliary devices, are intended to substitute for their disabled—such as by flooding—counterparts at a permanent substation [15]. Installing an MS may ordinarily require a couple of days but in a pinch can be accomplished within 24 hours [13], [15]. The kinds of connections permitted from an MS to a permanent one are described in [16]. For greater flexibility, some vendors of MSs allow transformers [15] and breakers [17], [18] to be transported on separate trailers instead of a single, long trailer.

Despite substituting for the most critical connections, MSs in aggregate often only furnish a minor portion of the total capacity of connections disabled in a large-scale flood event, such that restoration efforts remain the primary force behind recovery. Before such an event, it is common for repair crews to be staged on the outskirts of areas where weather forecasts indicate that damage is likely to occur [1], [14], [19], [20]. Staging considers not only the locations of pre-positioned personnel but also the quantity. If restoration is expected to require substantial labor, the affected utilities may rely on their mutual-assistance agreements with nearby utilities to call in additional crews [1], [14], [20]. Apart from the labor involved, outages may be inaccessible for repairs in the early days of a flood event due to submerged or obstructed roads [1], [13], [20], [21]. However, by deploying drones or riding helicopters, boats, and amphibious vehicles, crews can scout still-flooded areas to perform damage assessments that inform restoration planning [1], [14], [21].

In terms of flood damage from a hurricane, at a substation it is often the breakers and transformers that need to be repaired. A breaker that has been submerged should be completely disassembled for the removal of residue, corrosion, and deteriorated lubricants [11]. Then, mechanical parts of the breaker may be either reused or replaced, depending on attributes such as cost and existing wear from normal operation, but electronic parts (e.g., trip units and relays) should generally be replaced if the breaker is to be reconditioned [11], [22], [23]. Whether an electrical or conductive part can be reused often needs to be evaluated on an individual basis. As for transformers, it seems a dry-type transformer that has been submerged must almost invariably be replaced because the insulation will be compromised by water [22], [23].

Some sources [23] also insist that submerged liquid-filled transformers and cast-resin transformers be replaced, while other sources [22] suggest that such transformers stand a better chance of reconditioning.

Before a flood-damaged part of a component is reused, it must be subjected to a refurbishment process in which the part is thoroughly cleaned, dried, and tested [22], [24]. Methods, some of which can be administered on site in a matter of hours, for the refurbishment of motor and transformer windings are described in [24]. If a part cannot simply be returned to the manufacturer, then the refurbishment should be performed in consultation with the manufacturer by qualified personnel [22], [23], [24]. The personnel can be contracted from firms that specialize in electrical asset restoration [24], or they can be properly trained employees of the affected utility. Besides saving expense, the latter option avoids competition with other utilities for contracted services in the case of widespread flooding [24]. For improved readiness, a utility may also during normal times stockpile spare components or parts for rapid replacement of ones damaged in a flood event [24], [25]. A six-year pilot program led by the U.S. Department of Homeland Security (DHS) and the Electric Power Research Institute (EPRI) has successfully demonstrated the ''Recovery Transformer'' concept: with the proper design and preparedness, even a high-voltage power transformer can be installed and energized in less than six days [26].

B. COMPARISON TO PRIOR WORK

The stochastic MILP formulation of the present article is called the Transmission Restoration Problem with Mobile Substation Resources (TRP-MSR). To the knowledge of the authors, it is the first optimization model to account for MS resources, particularly within an optimal power flow. Nevertheless, provided in this subsection is a brief discussion of how it compares to some prior literature on optimizing the operational resilience of power systems, especially at the transmission level due to the nature of the TRP-MSR, but also at the distribution level. References in this subsection that address operational resilience but not explicitly at the distribution level can be assumed to address it at the transmission level.

A literature review on optimization models for emergency logistics in general, not just specifically for power systems, is [27]. According to this review, such models often combine stock pre-positioning and relief distribution, where the latter is commonly represented in terms of either commodity flow or resource allocation (vehicle routing constitutes both). The TRP-MSR aligns with these practices. Before the flood event, resources are pre-positioned at depots. Then, when a scenario of the event is realized, the LT dispatch of resources can be viewed as commodity flow, while the more flexible FT deployment of resources can be viewed as resource allocation.

Optimization models for operational transmission resilience may be deterministic [28], [29], [30], [31], [32], [33], [34], [35], [36], [37], [38] or stochastic [39], [40]. The TRP-MSR is a stochastic program. As in the referenced papers, stochastic models usually consist of two stages. Nevertheless, an example of a defender-attack-defender (D-A-D) robust program is provided in [41]. Another method, employed in the model of [42] for operational transmission resilience, to account for uncertainty is conditional value-at-risk. Still other modeling techniques to account for uncertainty, which have at least seen usage in models for operational distribution resilience, are chance-constrained programming [43] and distributionally robust programming [44]. The D-A-D structure [45], stochastic programming [46], [47], [48], [49], and deterministic programming [50], [51] are modeling methods leveraged for operational distribution resilience as well.

The representation of power flow is commonly a critical aspect of an optimization model for operational transmission resilience. The power-flow model most frequently employed at the transmission level is DC power flow [28], [29], [31], [35], [36], [38], [39], [40], [41], [52], which only considers real power. Alternatively, a nonlinear optimization model [32], [33], [36] may incorporate exact expressions for complex, AC power flow. A more practical representation to account for complex power is the LPAC model, which was introduced in [53], has been gaining traction for inclusion in transmission-resilience models [30], [34], and is adopted in the TRP-MSR. At the distribution level, the power-flow representation that tends to be employed is linearized DistFlow [54], [55], [56], as observed in the models of [45], [46], [48], [49], [50], and [51]. It is also possible that a generic network flow [47] be used at the distribution level (or the transmission level for that matter) that does not consider the dependence of flows on impedance.

When damage is modeled in operational transmission resilience, the cause of damage is often not directly considered [28], [31], [34], [38]. Otherwise, the cause tends to be hurricane wind, which is considered in conjunction with fragility models for grid components to generate damage scenarios [29], [35], [39], [40]. The models of [57] for fragility of grid components to wind are widely used, especially for operational distribution resilience [46], [47], but [47] references some other papers as well. (Alternatively, the cause of damage may not be directly considered at the distribution level either [45], [48], [49], [50], [51].) Still another method for producing damage cases may be simple, combinatorial generation [30]. Flood damage, especially over a multi-interval horizon as in the TRP-MSR, is not yet typically considered in optimization models for operational grid resilience. The models of [42] and [58], at the transmission and distribution levels respectively, are rare examples of ones that proactively account for final damage from a flood event. In the case of a D-A-D model, the damage is not incidental but deliberately orchestrated by a malicious attacker [41]. The deterministic, not D-A-D, optimization model of [52] is even more interesting in that it considers not how nature might threaten the transmission network, but how

transmission lines may be de-energized to lower the risk of causing wildfires.

A search for literature on optimal transmission-system restoration uncovers not only works accounting for the repair of damaged network components but also works on black-start (BS) restoration. Most works on black-start restoration [32], [33], [36], [37], [38] concern the re-energization of a transmission network following a complete blackout, but [38] is one of apparently few that also suppose components were damaged in the blackout event. On the contrary, since the TRP-MSR considers post-flood restoration over an extended, multi-day horizon, it is not a model suited for incorporating BS restoration but does involve repairs of flood-damaged substations.

In cases where optimal transmission-system restoration entails repairs [28], [29], [30], [31], [34], [35], [38], [39], [40], [52], the kinds of materials (e.g., parts) required for repairs are sometimes explicitly considered [28], [29], [40] but not in the TRP-MSR. Similar to [30], [31], [35], [38], [39], and [52], the TRP-MSR supposes that a pool of system-wide labor is allocated among repair tasks in each interval, but some works instead consider an available number of discrete crews, each of whose sequence of repair tasks over the horizon is explicitly scheduled [28], [29], [34]. The TRP-MSR assumes that each repair task requires a parametrized total amount of labor and that therefore the total duration required for completion of a repair task depends on how much labor is allocated to the task in each interval. In contrast, other models on operational transmission resilience may assume that a repair task is completed in a single interval [30], [35], [38], [52] or after a parametrized duration spanning multiple intervals [28], [29], [34]. The models of [31] and [39], which are among those that suppose a pool of system-wide restoration labor is allocated in each interval, have special assumptions about labor requirements for a repair task: completing a repair task requires a parametrized duration spanning multiple intervals, but allocation of labor to a task once the task is started must continue across intervals until it is completed. Representations of labor observed in papers on distribution resilience are similar to those in papers on transmission resilience. Moreover, in addition to repairing damaged components, crews at the distribution level may be responsible for visiting manual switches to open or close them [49]. Indeed, network reconfiguration in general seems more widely employed in distribution resilience [45], [46], [48], [49], [50], [51] than in transmission resilience. For computational tractability, network reconfiguration is not accounted for in the TRP-MSR.

As noted, the TRP-MSR is the first optimization model to consider MS resources. Although there already exist models for operational resilience considering other kinds of mobile power sources, such as mobile emergency generators [45], [46], [50] and mobile energy storage systems [45], [50], these models pertain to the distribution level, where the small capacities of mobile power sources would not limit their effectiveness. As in the TRP-MSR, repair crews also constitute a kind of mobile resource, at both the transmission level [28], [29], [30], [31], [34], [35], [38], [39], [52] and the distribution level [47], [48], [49], [50], [51]. At both the transmission level [31], [39] and the distribution level [45], mobile resources may be pre-positioned directly at components. They may also be pre-positioned at depots, as observed in distribution resilience [46], [47], [49] and likely also in transmission resilience. Like other resources, restoration labor that is represented as distinct crews in transmission resilience may be individually routed between locations [28], [29], [34]. Crews that are routed are usually required to return to depots at the end of the horizon [28], [29], [34].

Often, operational-resilience models that are multi-interval are deterministic [28], [29], [30], [31], [32], [33], [34], [35], [36], [37], [38], [52]. When two-stage stochastic programs are multi-interval, they are sometimes multi-interval only in the second stage, as is the case for the TRP-MSR and exemplified by the model of [48] for distribution resilience. The stochastic program of [39] for transmission resilience is interesting in that the first stage pre-allocates restoration resources over a multi-interval horizon, while the second stage allocates more restoration resources over the same horizon. The stochastic program of [49] for distribution resilience is also unique: both the first and second stages consider multi-interval horizons since the first stage routes crews to operate manual switches before the disaster event. The transmission-resilience model of [41] is a special example of a D-A-D robust program with a multi-interval horizon: attacks are characterized not just by their target components but also by timing.

Optimization models for operational transmission resilience can be single-objective or multi-objective. In the case of a single objective, the objective may be to minimize the (weighted) load shed [29], [30], [33], [37], [38], [40], maximize the (weighted) picked-up discrete loads [28], [32], [36], or minimize a sum of multiple kinds of costs [31], [35], [39], [41], [47] as in the TRP-MSR. Multi-objective models have the multiple, incompatible objectives scaled by different multipliers and then summed together. An example of two objectives in transmission resilience is to simultaneously minimize the load-interruption cost and minimize the total time to repair components [34]. Another example is to simultaneously maximize the load served, minimize wildfire risk, and minimize grid vulnerability [52]. Interesting cases of multiple objectives can also be found at the distribution level. One example is to simultaneously maximize the picked-up loads and minimize the number of travels of mobile resources [50]. A second example is to simultaneously maximize the picked-up loads and minimize the weighted sum of outage durations of loads [51].

To improve the computational tractability of a model for operational transmission resilience, one simple method is to break the model down into a pipeline of subproblems [29], [33], [36], [37], where the solution values of one subproblem in the pipeline are inputs into another

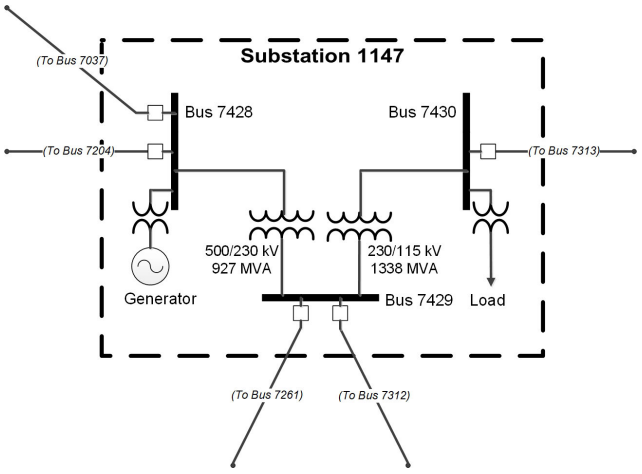

FIGURE 1. Network elements and connection sites within a transmission substation.

subproblem. For a D-A-D robust program, a column-and-constraint generation algorithm [41] may be used to solve the model more efficiently. For a stochastic program, strategies used include Benders' decomposition [39], a custom column-generation algorithm [40], and a custom branch-and-cut algorithm [32], the last of which is only applicable for mixed-integer stochastic programs. Progressive hedging is another strategy observed to efficiently solve stochastic programs, for distribution resilience [47], [48] and likely also for transmission resilience. Notably, Benders' decomposition cannot be applied to stochastic programs with integer variables in the second stage, and the TRP-MSR is such a stochastic program.

C. ORGANIZATION OF THE ARTICLE

The rest of this article is organized as follows. Section II presents the stochastic MILP formulation referred to as the Transmission Restoration Problem with Mobile Substation Resources (TRP-MSR). Section III introduces the parallel heuristic designed to efficiently solve the problem. Section IV describes the setup of experiments validating the formulation. Section V discusses results and lessons learned from these experiments. Section VI concludes with closing remarks.

II. MATHEMATICAL OPTIMIZATION MODEL

This section describes the stochastic MILP model developed to coordinate MS resource deployment and permanent-substation restoration in the face of a widespread flood event.

A. OVERVIEW

1) SPATIAL CONSIDERATIONS

The transmission system is depicted as consisting of a set of substations $\mathcal{N}$. As depicted in Fig. 1, each transmission substation contains a group of buses connected by branch transformers. If any two substations are connected, it is through a transmission line between a bus within the first substation and a bus within the other. A substation also contains the connections at its buses. The following are the types of connections that may be found at a bus: generation step-up, primary-distribution step-down, the origin of a transmission line, and the destination of a transmission line. In contrast, if a branch transformer exists, it constitutes a connection not solely associated with any single bus at the substation. Transmission line origin and destination connections are described with one-sided voltage ratings and can be substituted with mobile breakers. Generation step-up connections, primary-distribution step-down connections, and branch transformers are described with two-sided voltage ratings and can be substituted with mobile transformers.

In the stochastic MILP model, the sets of connection sites having two-sided and one-sided voltage ratings are denoted by Ξ and Γ, respectively. For convenience, e_ξ can signify any of $e_{i,\mathrm{G}}$, $e_{i,\mathrm{L}}$, and e_x, while a_γ can signify either of $a_{l,\mathrm{O}}$ and $a_{l,\mathrm{D}}$. Due to the negligible footprint of a substation compared to a transmission line, the buses and their connections are viewed as sharing the same geographical coordinates. Thus, when a substation is disabled by flooding in a scenario, all connections at the substation are disabled, though the buses themselves are assumed to remain intact. While the control cabinets of substation breakers and transformers are commonly no more than a meter above ground [8], [9], substation busbars and power lines even at the distribution level are generally supported at heights of at least 10 feet [7]. Alternatively, temporary buses may be raised just outside the substation.

From a spatial perspective, the model also assumes a set of depots $\mathcal{Z}$ at which MS resources can be staged before the event. For each depot, there exists a set of substations that the depot can reach even during times of limited traversability on the road network spanning the transmission system.

2) TEMPORAL CONSIDERATIONS

The time horizon consists of a set of intervals $\mathcal{T}$ of uniform duration. The interval duration must be at least 24 hours to allow the assumption that an MS resource can be transported and fully energized in a single interval. Furthermore, the horizon of a scenario is divided into two periods: the period of *limited traversability* (LT) $\mathcal{T}^s_{\mathrm{LT}}$ and that of *full traversability* (FT) $\mathcal{T}^s_{\mathrm{FT}}$. During the LT period, MS resources staged at a depot can only be dispatched to and deployed at accessible substations reachable from the depot. During the FT period, MS resources can be deployed at all accessible substations regardless of where the resources were staged before the event, and accessible substations can accumulate restoration labor to be reinstated.

In terms of parametrization, two aspects of the state of a substation are considered to vary over the course of the horizon: (i) disabling by flooding and (ii) accessibility. A substation is deemed *disabled* by flooding starting with the first interval in which the flood height at the substation exceeds some threshold, which in practice may be the height of control cabinets at the substation. Thus, parameters O^{st}_n and

R_n^{st} are related by the expression $1 - O_n^{st} = \prod_{t_1=1}^{t}(1 - R_n^{s,t_1})$. In an interval of a scenario, a substation is deemed *accessible* to MS resources and restoration if and only if the flood height is below the disabling threshold in the present interval and will not exceed it in a later interval. If the flood height is not presently above the threshold but will be in a later interval, then the substation is deemed inaccessible. By this definition of accessibility, parameter Ω_n^{st} has value $\prod_{t_1=t}^{|\mathcal{T}|}(1 - R_n^{s,t_1})$.

B. STOCHASTIC MILP FORMULATION

The stochastic MILP model developed is

$$\min \quad j_{\mathrm{ST}} + \sum_{s\in\mathcal{S}} \Upsilon_s(j_{s,\mathrm{IN}} + j_{s,\mathrm{G}} + j_{s,\mathrm{L}}), \tag{1}$$

subject to

$$\text{(a) } j_{\mathrm{ST}} = \sum_{z\in\mathcal{Z}}\Big(\sum_{w\in\mathcal{W}} \Psi_{zw} e_{zw} + \sum_{u\in\mathcal{U}} \Psi_{zu} a_{zu}\Big), \tag{2}$$

$$\forall s \in \mathcal{S}, \quad \text{(b) } j_{s,\mathrm{IN}} = \sum_{t\in\mathcal{T}}\Bigg(\sum_{x\in\mathcal{X}} \acute{\Psi}_x^s \acute{e}_x^{st} + \sum_{i\in\mathcal{I}} \big(\acute{\Psi}_{i,\mathrm{T}}^s(\acute{e}_{i,\mathrm{G}}^{st} + \acute{e}_{i,\mathrm{L}}^{st}) + \acute{\Psi}_{i,\mathrm{B}}^s\Big(\sum_{l\in\mathcal{L}|o(l)=i} \acute{a}_{l,\mathrm{O}}^{st} + \sum_{l\in\mathcal{L}|d(l)=i} \acute{a}_{l,\mathrm{D}}^{st}\Big)\Big)\Bigg),$$

$$\text{(c) } j_{s,\mathrm{G}} = \Delta t \sum_{t\in\mathcal{T}}\sum_{i\in\mathcal{I}} \Phi_{i,\mathrm{G}}^{st} p_{i,\mathrm{G}}^{st},$$

$$\text{(d) } j_{s,\mathrm{L}} = \Delta t \sum_{t\in\mathcal{T}}\sum_{i\in\mathcal{I}} \Phi_{i,\mathrm{L}}^{st} h_i^{st},$$

$$\text{(a) } \forall u \in \mathcal{U}, \sum_{z\in\mathcal{Z}} a_{zu} \le A_u, \quad \text{(b) } \sum_{z\in\mathcal{Z}}\sum_{u\in\mathcal{U}} a_{zu} \le A_{\mathrm{TTL}}, \tag{3}$$

$$\text{(c) } \forall w \in \mathcal{W}, \sum_{z\in\mathcal{Z}} e_{zw} \le E_w,$$

$$\text{(d) } \sum_{z\in\mathcal{Z}}\sum_{w\in\mathcal{W}} e_{zw} \le E_{\mathrm{TTL}},$$

$$\text{(a) } \forall s \in \mathcal{S}, \forall t \in \mathcal{T}_{\mathrm{FT}}^s, \quad \sum_{n\in\mathcal{N}} y_n^{st} \le \overline{Y}^{st}, \tag{4}$$

$$\forall s \in \mathcal{S}, \forall n \in \mathcal{N}, \quad \text{(b) } \forall t \in \mathcal{T}_{\mathrm{LT}}^s, \quad y_n^{st} = 0,$$

$$\text{(c) } \forall t \in \mathcal{T}_{\mathrm{FT}}^s, \quad 0 \le y_n^{st} \le \overline{Y}_n^{st}\Omega_n^{st}(1 - \hat{\mu}_n^{st}),$$

$$\text{(d) } \forall t \in \mathcal{T}, \quad \Psi_n^s(1 - \mu_n^{st}) + \sum_{t_1=1}^{t-1} y_n^{s,t_1} \ge \Psi_n^s,$$

$$\text{(e) } \forall t \in \mathcal{T}, \quad (\sum_{t_1=1}^{t-1} \overline{Y}_n^{s,t_1})\mu_n^{st} + \Psi_n^s - \epsilon \ge \sum_{t_1=1}^{t-1} y_n^{s,t_1},$$

$$\text{(f) } \forall t \in \mathcal{T}, \quad 1 - \hat{\mu}_n^{st} = O_n^{st}(1 - \mu_n^{st}),$$

$$\forall s \in \mathcal{S}, \forall z \in \mathcal{Z}, \tag{5}$$

$$\text{(a) } \forall u \in \mathcal{U}, \sum_{t\in\mathcal{T}_{\mathrm{LT}}^s}\Big(\sum_{l\in\mathcal{L}_{u,\mathrm{O}}} a_{zl,\mathrm{O}}^{st} + \sum_{l\in\mathcal{L}_{u,\mathrm{D}}} a_{zl,\mathrm{D}}^{st}\Big) \le a_{zu},$$

$$\text{(b) } \forall w \in \mathcal{W}, \sum_{t\in\mathcal{T}_{\mathrm{LT}}^s}\Big(\sum_{i\in\mathcal{I}_{w,\mathrm{G}}} e_{zi,\mathrm{G}}^{st} + \sum_{i\in\mathcal{I}_{w,\mathrm{L}}} e_{zi,\mathrm{L}}^{st} + \sum_{x\in\mathcal{X}_w} e_{zx}^{st}\Big) \le e_{zw},$$

$$\text{(c) } \forall t \in \mathcal{T}_{\mathrm{LT}}^s, \forall \gamma \in \Gamma, \quad a_{z\gamma}^{st} \le K_{z,n(\gamma)}\Omega_{n(\gamma)}^{st}(1 - \hat{\mu}_{n(\gamma)}^{st}),$$

$$\text{(d) } \forall t \in \mathcal{T}_{\mathrm{LT}}^s, \forall \xi \in \Xi \setminus \mathcal{X}, \quad e_{z\xi}^{st} \le E_{\mathrm{TTL}} K_{z,n(\xi)}\Omega_{n(\xi)}^{st}(1 - \hat{\mu}_{n(\xi)}^{st}),$$

$$\text{(e) } \forall t \in \mathcal{T}_{\mathrm{LT}}^s, \forall x \in \mathcal{X}, \quad e_{zx}^{st} \le E_{\mathrm{TTL}} K_{z,n(x)}\Omega_{n(x)}^{st}$$

$$\forall s \in \mathcal{S}, \forall t \in \mathcal{T}_{\mathrm{LT}}^s, \text{ (f) } \forall \gamma \in \Gamma, \ a_\gamma^{st} \le \sum_{t_1=1}^{t}\sum_{z\in\mathcal{Z}} a_{z\gamma}^{s,t_1},$$

$$\text{(g) } \forall \xi \in \Xi, \quad e_\xi^{st} \le \sum_{t_1=1}^{t}\sum_{z\in\mathcal{Z}} e_{z\xi}^{s,t_1}, \forall s \in \mathcal{S}, \forall t \in \mathcal{T}_{\mathrm{FT}}^s,$$

$$\text{(a) } \forall \gamma \in \Gamma, a_\gamma^{st} \le \Omega_{n(\gamma)}^{st}(1 - \hat{\mu}_{n(\gamma)}^{st}), \tag{6}$$

$$\text{(b) } \forall \xi \in \Xi \setminus \mathcal{X}, \quad e_\xi^{st} \le E_{\mathrm{TTL}}\Omega_{n(\xi)}^{st}(1 - \hat{\mu}_{n(\xi)}^{st}),$$

$$\text{(c) } \forall x \in \mathcal{X}, \quad e_x^{st} \le E_{\mathrm{TTL}}\Omega_{n(x)}^{st},$$

$$\text{(d) } \forall u \in \mathcal{U}, \quad \sum_{l\in\mathcal{L}_{u,\mathrm{O}}} a_{l,\mathrm{O}}^{st} + \sum_{l\in\mathcal{L}_{u,\mathrm{D}}} a_{l,\mathrm{D}}^{st} \le \sum_{z\in\mathcal{Z}} a_{zu},$$

$$\text{(e) } \forall w \in \mathcal{W}, \sum_{i\in\mathcal{I}_{w,\mathrm{G}}} e_{i,\mathrm{G}}^{st} + \sum_{i\in\mathcal{I}_{w,\mathrm{L}}} e_{i,\mathrm{L}}^{st} + \sum_{x\in\mathcal{X}_w} e_x^{st} \le \sum_{z\in\mathcal{Z}} e_{zw},$$

$$\forall s \in \mathcal{S}, \forall \gamma \in \Gamma, \quad \text{(a) } \hat{a}_\gamma^{s1} = 0, \tag{7}$$

$$\text{(b) } \forall t \in \mathcal{T} | t > 1, \quad \hat{a}_\gamma^{st} = a_\gamma^{s,t-1} a_\gamma^{st},$$

$$\text{(c) } \forall t \in \mathcal{T} | t > 1, \quad \acute{a}_\gamma^{st} = (1 - a_\gamma^{s,t-1}) a_\gamma^{st},$$

$$\forall s \in \mathcal{S}, \forall \xi \in \Xi, \quad \text{(d) } \hat{e}_\xi^{s1} = 0,$$

$$\text{(e) } \forall t \in \mathcal{T} | t > 1, \quad \hat{e}_\xi^{st} \le \min\{e_\xi^{st}, e_\xi^{s,t-1}\},$$

$$\text{(f) } \forall t \in \mathcal{T} | t > 1, \quad \acute{e}_\xi^{st} \ge \max\{0, e_\xi^{st} - e_\xi^{s,t-1}\},$$

$$\forall s \in \mathcal{S}, \forall t \in \mathcal{T}, \forall l \in \mathcal{L}, \quad \text{(a) } \hat{\sigma}_l^{st} = \sigma_{l,\mathrm{O}}^{st}\sigma_{l,\mathrm{D}}^{st}, \tag{8}$$

$$\text{(b) } 1 - \sigma_{l,\mathrm{O}}^{st} = (1 - \hat{\mu}_{n(o(l))}^{st})(1 - \hat{a}_{l,\mathrm{O}}^{st}),$$

$$\text{(c) } 1 - \sigma_{l,\mathrm{D}}^{st} = (1 - \hat{\mu}_{n(d(l))}^{st})(1 - \hat{a}_{l,\mathrm{D}}^{st}),$$

$$\forall s \in \mathcal{S}, \forall t \in \mathcal{T}, \forall x \in \mathcal{X}, \text{(d) } (E_{\mathrm{TTL}} + 1)\hat{\sigma}_x^{st} \ge \hat{e}_x^{st} + \hat{\mu}_{n(x)}^{st},$$

$$\text{(e) } \hat{\sigma}_x^{st} \le \hat{e}_x^{st} + \hat{\mu}_{n(x)}^{st},$$

$$\text{(a) } \forall s \in \mathcal{S}, \forall t \in \mathcal{T}_{\mathrm{FT}}^s, \forall i \in \mathcal{I}, \quad d_i^{st} \ge d_i^{s,t-1}, \tag{9}$$

$$\forall s \in \mathcal{S}, \forall t \in \mathcal{T}, \forall i \in \mathcal{I}, \quad \text{(b) } v_i^{st} = \ddot{V}_i + \eta_i^{st},$$

$$\text{(c) } \underline{V}_i \le v_i^{st} \le \overline{V}_i,$$

$$\text{(d) } \sum_{\lambda'\in\Lambda'|o(\lambda')=i} p_{\lambda'}^{st} = p_{i,\mathrm{G}}^{st} - d_i^{st},$$

$$\text{(e) } \sum_{\lambda'\in\Lambda'|o(\lambda')=i} q_{\lambda'}^{st} = q_{i,\mathrm{G}}^{st} - f_i^{st}, \quad \text{(f) } 0 \le \zeta_i^{st} \le 1,$$

$$\text{(g) } h_i^{st} = D_i^{st}\zeta_i^{st}, \text{ (h) } d_i^{st} = D_i^{st} - h_i^{st},$$

$$\text{(i) } f_i^{st} = F_i^{st}(1 - \zeta_i^{st}),$$

$$\forall s \in \mathcal{S}, \forall t \in \mathcal{T}, \tag{10}$$
$$\text{(a)}\ \forall \lambda' \in \Lambda', \quad \delta^{st}_{\lambda'} = \theta^{st}_{o(\lambda')} - \theta^{st}_{d(\lambda')},$$
$$\text{(b)}\ \forall \lambda' \in \Lambda', \quad -\overline{\delta} \le \delta^{st}_{\lambda'} \le \overline{\delta},$$
$$\text{(c)}\ \forall \lambda \in \Lambda, \quad \underline{COS} \le cos^{st}_{\lambda} \le \overline{COS},$$
$$\forall s \in \mathcal{S}, \forall t \in \mathcal{T}, \forall \lambda' \in \Lambda', \tag{11}$$
$$\text{(a)}\ \ddot{V}^2_{o(\lambda')} G_{\nu(\lambda')} - \ddot{V}_{o(\lambda')} \ddot{V}_{d(\lambda')} (G_{\nu(\lambda')} cos^{st}_{\nu(\lambda')} + B_{\nu(\lambda')} \delta^{st}_{\lambda'}) - p^{st}_{\lambda'} \le M(1 - \hat{\sigma}^{st}_{\nu(\lambda')}),$$
$$\text{(b)}\ \cdots, \quad \text{(c)}\ \cdots, \quad \text{(d)}\ \cdots,$$
$$\forall s \in \mathcal{S}, \forall t \in \mathcal{T}, \tag{12}$$
$$\text{(a)}\ \forall \lambda' \in \Lambda', -\hat{\sigma}^{st}_{\nu(\lambda')} \le \frac{1}{M} p^{st}_{\lambda'} \le \hat{\sigma}^{st}_{\nu(\lambda')},$$
$$\text{(b)}\ \forall \lambda' \in \Lambda', \quad -\hat{\sigma}^{st}_{\nu(\lambda')} \le \frac{1}{M} q^{st}_{\lambda'} \le \hat{\sigma}^{st}_{\nu(\lambda')},$$
$$\text{(c)}\ \forall l' \in \mathcal{L}', \quad (p^{st}_{l'})^2 + (q^{st}_{l'})^2 \le \overline{S}^2_{\nu(l')},$$
$$\text{(d)}\ \forall w \in \mathcal{W}, \forall x' \in \mathcal{X}'_w,$$
$$(p^{st}_{x'})^2 + (q^{st}_{x'})^2 \le (S_{w,\mathrm{T}} \hat{e}^{st}_{\nu(x')} + \overline{S}_{\nu(x')} \hat{\mu}^{st}_{n(\nu(x'))})^2,$$
$$\forall s \in \mathcal{S}, \forall t \in \mathcal{T}, \tag{13}$$
$$\text{(a)}\ \forall i \in \mathcal{I}, 0 \le p^{st}_{i,\mathrm{G}} \le \overline{P}^s_i (1 - O^{st}_{i,\mathrm{GM}}),$$
$$\text{(b)}\ \forall i \in \mathcal{I},$$
$$\underline{Q}^s_i (1 - O^{st}_{i,\mathrm{GM}}) \le q^{st}_{i,\mathrm{G}} \le \overline{Q}^s_i (1 - O^{st}_{i,\mathrm{GM}}),$$
$$\text{(c)}\ \forall w \in \mathcal{W}, \forall i \in \mathcal{I}_{w,\mathrm{G}},$$
$$(p^{st}_{i,\mathrm{G}})^2 + (q^{st}_{i,\mathrm{G}})^2 \le (S_{w,\mathrm{T}} \hat{e}^{st}_{i,\mathrm{G}} + \overline{S}_{i,\mathrm{G}} \hat{\mu}^{st}_{n(i)})^2,$$
$$\text{(d)}\ \forall w \in \mathcal{W}, \forall i \in \mathcal{I}_{w,\mathrm{L}},$$
$$(d^{st}_i)^2 + (f^{st}_i)^2 \le (S_{w,\mathrm{T}} \hat{e}^{st}_{i,\mathrm{L}} + \overline{S}_{i,\mathrm{L}} \hat{\mu}^{st}_{n(i)})^2.$$

The objective (1) is to minimize the sum of the cost of (i) MS resource staging and the expected costs of (ii) MS resource installation, (iii) real power generation, and (iv) real load shed. Constraints (2) provide the expressions for these costs. As seen in Constraint (2b), an installation cost is incurred whenever a resource is newly installed at a connection site.

Constraints (3) enforce allowances for the staging of two kinds of MS resources: mobile transformers (MTs) and mobile breakers (MBs). For each kind of resource, the total quantity across voltage ratings cannot exceed a total allowance, and there also exist rating-specific allowances.

Constraints (4) capture whether substations are reinstated or operational. Restoration of a substation disabled by flooding can only occur in an FT interval, and only if the substation is both disabled and accessible in that interval. In each FT interval, there is a system-wide amount of restoration labor that can be allocated among disabled substations, and at each substation there is also a limit on the amount of labor that can be allocated to it. A disabled substation is reinstated if it has accumulated sufficient restoration labor in previous intervals. In an interval, a substation is operational if and only if it is either (i) reinstated or (ii) not yet disabled by flooding.

Constraints (5) concern deployment of resources during the LT period of each scenario. During the LT period, a resource staged at a depot can only be dispatched once. The connection site to which the resource is dispatched must be at a substation reachable from the depot, and the dispatch must occur in an interval that the substation is accessible. Starting in the interval that the resource is dispatched to the site, the resource is considered deployed at the site. An MT can be dispatched to augment a branch transformer within a substation that is operational. For other kinds of connection sites, resources cannot be dispatched to sites within operational substations.

Constraints (6) concern deployment of resources during the FT period of each scenario. Unlike during the LT period, the sites at which a resource can be deployed do not depend on the depot at which the resource was staged before the event. Nevertheless, as during the LT period, resources cannot be deployed at sites within inaccessible substations, and the deployment of MTs at branch transformers is the only case where resources can be deployed at sites within operational substations.

Constraints (7) track whether resources are operational or newly installed. In an interval, a resource is operational at a site if and only if the resource (i) was deployed at the site in the previous interval and (ii) continues to be deployed at the site. A resource is newly installed at a site if and only if the resource (i) was not deployed at the site in the previous interval and (ii) is now deployed at the site. A nonlinear equality constraint involving a product of binary-valued variable expressions, such as Constraint (7c), is linearized exactly as multiple inequality constraints by McCormick relaxation.

Constraints (8) capture whether branches are operational. A line is operational if and only if both ends of the line are operational. The connection at an end of a line is operational if and only if either (i) the substation containing the bus of the connection is operational or (ii) an MB is operational at the connection. Likewise, a branch transformer is operational if and only if either (i) the substation containing it is operational or (ii) at least one MT is operational at the branch transformer.

Constraints (9) account for various aspects of bus operation: voltage magnitude, load shed, and power balance. It should be noted that during the FT period, since no substations are newly flooded, Constraint (9a) forbids load supplied at a bus in an interval to decrease from the previous interval.

Constraints (10) account for voltage angle differences across branches, while constraints (11) provide expressions for real and reactive flows in branches. All of the constraints in these two groups are based on the LPAC model [53]. Constraints (12) account for the capacities of branches. Constraints (13) account for generator capacities and for the capacities of generation step-up and primary-distribution step-down connections. A constraint, such as Constraint (12d), corresponding to a disc feasible region with variable radius would be achieved exactly by a second-order

cone constraint. However, such a region is approximated by an intersection of halfspaces specified by linear inequality constraints.

III. PARALLEL HEURISTIC

This section outlines the parallel heuristic designed to efficiently solve the TRP-MSR. The heuristic is based on a concept of formations that is also described in this section.

A. GENERAL REMARKS

The inputs to Algorithm 1 (i.e., the top level of the heuristic) are maximum decomposition iterations J, expected (i.e., stochastic) objective tolerance E, horizon-level perturbations H, count divisor C, interval-level perturbations V, and locational dispersion D. At the end of Algorithm 1, a complete heuristic solution to the TRP-MSR instance is returned. Algorithm 2 is one of the subroutines of Algorithm 1, while Algorithm 3 is one of the subroutines of Algorithm 2. Once a subroutine produces a solution, the solution is not altered by the algorithm that invoked the subroutine. All three algorithms and their subroutines are assumed to have full access to the problem parameters of the TRP-MSR instance; accordingly, the problem parameters are not listed as arguments to the functions for the algorithms and for their subroutines. Within each algorithm, any for loop over the set of scenarios $\mathcal{S}$ can have its iterations execute in parallel, but the fork-join paradigm requires that every scenario's iteration finish executing before the instructions after the for loop begin serial execution. Additionally, the subproblems (e.g., `RestSeqProb`) commonly optimize continuous variables that are variants of the following ones for LPAC-based optimal power flow: $j_{s,\mathrm{G}}$, $j_{s,\mathrm{L}}$, h_i^{st}, η_i^{st}, v_i^{st}, θ_i^{st}, $p_{i,\mathrm{G}}^{st}$, $q_{i,\mathrm{G}}^{st}$, d_i^{st}, f_i^{st}, ζ_i^{st}, cos_λ^{st}, $\delta_{\lambda'}^{st}$, $p_{\lambda'}^{st}$, and $q_{\lambda'}^{st}$.

B. ALGORITHM 1: TOP LEVEL OF HEURISTIC

The following steps are performed in Algorithm 1.

(I) For each scenario, solve an instance of the restoration-sequencing problem (abbreviated as `RestSeqProb`), which decides the allocation of restoration labor, but not MS resource deployment, over the scenario's FT period while accounting for optimal power flow.
- The `RestSeqProb` supposes that no MS resources are available for pre-selection and pre-positioning before the event. Thus, the `RestSeqProb` is effectively a variant of the TRP-MSR that considers a single scenario and has MS resource allowances of zero. However, the objective function of the `RestSeqProb` is the sum of the costs of real power generation and real load shed, as MS resources are not modeled.
- Specifically, the `RestSeqProb` optimizes restoration variables that are variants of y_n^{st}, μ_n^{st}, $\hat{\mu}_n^{st}$, $\hat{\sigma}_\lambda^{st}$, $\sigma_{l,\mathrm{O}}^{st}$, and $\sigma_{l,\mathrm{D}}^{st}$, as well as variants of the variables for optimal power flow that are listed in Section III-A. Moreover, only by one scenario s and values of t within the FT period $\{|\mathcal{T}_{\mathrm{LT}}^s|+1, \ldots, |\mathcal{T}|\}$ are variables indexed. The solution values of y_n^{st}, μ_n^{st}, and $\hat{\mu}_n^{st}$ can be called the restoration values.
- Once the restoration values are determined for each scenario, they remain unchanged for the lifetime of the heuristic.

(II) Execute Algorithm 2 to, considering the restoration values, decide the pre-selection—but not pre-positioning—of MS resources.

(III) Solve the solution-completion problem (abbreviated as `SolCompProb`), which is a variant of the TRP-MSR that, still stochastic, completes the heuristic solution by deciding the pre-positioning, LT dispatch, and FT deployment of MS resources, as well as the power-flow operations. Specifically, the `SolCompProb` optimizes—with an objective function still given by the sum of the costs of MS resource staging, MS resource installation, real power generation, and real load shed—variants of all variables except y_n^{st}, μ_n^{st}, and $\hat{\mu}_n^{st}$. For the variables optimized, all indices are considered.

Algorithm 1 Top Level of Heuristic

Input: J, E, H, C, V, D
Output: *heurSol*
1: *restVals* ← {}
2: **for all** $s \in \mathcal{S}$ **do**
3: *restVals*[s] ← `RestSeqProb`(s)
4: **end for**
5: *resoSelSol* ← `Algorithm2`(J, E, H, C, V, D, *restVals*)
6: *heurSol* ← `SolCompProb`(*restVals*, *resoSelSol*)
7: **return** *heurSol*

C. ALGORITHM 2: UPPER LEVEL OF DECOMPOSITION

Algorithm 2 is essentially a decomposition method, where what changes between iterations j is the MS resource pre-selection. In each iteration, the following steps are performed.

(I) For each scenario, solve an instance of the horizon-level MS resource deployment problem (abbreviated as `HResoDepProb`) considering the scenario's restoration values and the MS resources pre-selected by step (IV) of the previous decomposition iteration. Execute `GetObj` to collect the objective value of a scenario's `HResoDepProb` instance.
- The `HResoDepProb`, which pre-selects MS resources and optimizes their deployment over the scenario's FT period, is a variant of the TRP-MSR that considers a single scenario and has restoration values fixed. The objective function of the `HResoDepProb` is the sum of the costs of MS resource installation, real power generation, and real load shed because the pre-positioning of MS resources at depots is not modeled.
- Specifically, the `HResoDepProb` optimizes variants of the variables $j_{s,\mathrm{IN}}$, $a_{l,\mathrm{O}}^{st}$, $a_{l,\mathrm{D}}^{st}$, $\hat{a}_{l,\mathrm{O}}^{st}$, $\hat{a}_{l,\mathrm{D}}^{st}$, $\acute{a}_{l,\mathrm{O}}^{st}$, $\acute{a}_{l,\mathrm{D}}^{st}$, e_x^{st}, $\hat{e}_x^{st}$, $\acute{e}_x^{st}$, $e_{i,\mathrm{G}}^{st}$, $e_{i,\mathrm{L}}^{st}$, $\hat{e}_{i,\mathrm{G}}^{st}$, $\hat{e}_{i,\mathrm{L}}^{st}$, $\acute{e}_{i,\mathrm{G}}^{st}$, $\acute{e}_{i,\mathrm{L}}^{st}$, $\hat{\sigma}_\lambda^{st}$, $\sigma_{l,\mathrm{O}}^{st}$, and $\sigma_{l,\mathrm{D}}^{st}$, as well as variants of the variables for optimal

power flow that are listed in Section III-A. In place of a_{zu} and e_{zw}, the HResoDepProb optimizes variables for MS resource pre-selection that are indexed only by voltage rating. Moreover, only by one scenario s and values of t within the FT period $\{|\mathcal{T}^s_{\mathrm{LT}}|+1,\ldots,|\mathcal{T}|\}$ are variables indexed.

- The arguments to the function for the HResoDepProb are normally the scenario s, the locational dispersion D, the restoration values of scenario s as they are given by *restVals*[s], the pre-selection of MS resources as given by *resoSelSol*, and the solutions of previous HResoDepProb instances for scenario s as they are given by *hResoDepSols*[s].
- However, as the HResoDepProb instance here is the first for its scenario, there are no previous HResoDepProb instances whose solutions the HResoDepProb instance here must take into account. Accordingly, NULL is specified in place of *hResoDepSols*[s], and 0 is specified in place of D.
- The pre-selection of MS resources must be such that the quantity for a kind (i.e., MT or MB) and voltage rating does not differ by more than some fixed positive integer (e.g., 1) from its quantity in *resoSelSol*, which contains the pre-selection decided by step (IV) of the previous decomposition iteration.
- It is critical to note though that for each scenario, the HResoDepProb instance of the first decomposition iteration (i.e., iteration $j=1$) is free to pre-select MS resources within allowances.

(II) With the scenario objective values, execute CalcExpObj to calculate an expected objective value. Then, if the maximum number of complete decomposition iterations J has already been executed, or if the expected objective value's percent change from that of the previous decomposition iteration is no more than tolerance $E\times 100\%$, consider the decomposition method to have converged. In such a case, without proceeding to steps (III) and (IV), return the MS resource pre-selection decided by step (IV) of the previous decomposition iteration.

(III) For each scenario, execute Algorithm 3 to identify and analyze MS resource deployment formations. The significance of formations is explained in Section III-D.

(IV) Considering the formations for each scenario, solve the resource-selection problem (abbreviated as ResoSelProb) to decide a pre-selection of MS resources. The ResoSelProb is not a variant of the TRP-MSR but is given in Section III-D.

D. CONCEPT OF FORMATIONS

For each scenario, since Algorithm 1 solves the RestSeqProb, algorithms 2 and 3 see the progression of permanent-substation restoration over the scenario's FT period as fixed. Therefore, the idea of the formations concept is to determine in each FT interval, accounting for optimal power flow, what configurations of operational (as captured by $\hat{a}^{st}_{\gamma}$ or $\hat{e}^{st}_{\xi}$) MS resources would yield the most improvement in the objective value beyond just the mere progression of permanent-substation restoration. The calculated improvement in the objective value is viewed as a reduction of total cost and is called the *relief benefit*. Moreover, a *formation* is defined as a tuple of quantities of operational MS resources at the set of connection sites within a transmission network. (Then, to facilitate conceptualization, one may view the relief benefit of a formation as capturing an improvement relative to the total cost of a "null formation" involving no operational MS resources.)

One formation can be considered a *sub-formation* of a second formation if, within the transmission network, there exists no connection site at which the first formation has a greater resource quantity than the second formation does. The overall strategy of Algorithm 2 is to ultimately pre-select MS resources such that the formations whose construction is enabled—across all the FT intervals of all the scenarios—yield the greatest expected total relief benefit. If, in an FT interval of a scenario, the ideal formation would not be convenient to construct in terms of MS resource requirements, perhaps much of the formation's relief benefit could still be gained by construction of a vital sub-formation. An example of the concept is provided in Section V-C.

With the assumption that MS resource staging and installation costs are negligible, the ResoSelProb solved in step (IV) of each decomposition iteration is given by

$$\text{(a)}\ \max \sum_{s\in\mathcal{S}} \Upsilon_s \sum_{t\in\mathcal{T}^s_{\mathrm{FT}}} \sum_{f\in\mathcal{F}_{st}} \Delta_{stf}\,\rho_{stf} \tag{14}$$

subject to

Algorithm 2 Upper Level of Decomposition

Input: J, E, H, C, V, D, *restVals*
Output: *resoSelSol*

$j \leftarrow 1$; *converged* $\leftarrow$ FALSE; *resoSelSol* $\leftarrow$ NULL
oldObj $\leftarrow 1/\infty$; *newObj* $\leftarrow 0$
while *converged* $=$ FALSE **do**
  objs $\leftarrow \{\}$; *hResoDepSols* $\leftarrow \{\}$; *formDescs* $\leftarrow \{\}$
  for all $s \in \mathcal{S}$ **do**
    hResoDepSols[s] $\leftarrow \{\}$
    hResoDepSols[s][1] $\leftarrow$ HResoDepProb(s, 0, *restVals*[s], *resoSelSol*, NULL)
    objs[s] $\leftarrow$ GetObj(*hResoDepSols*[s][1])
  end for
  newObj $\leftarrow$ CalcExpObj(*objs*)
  converged $\leftarrow (j = J+1)$ or $\left(\frac{|newObj-oldObj|}{|oldObj|} \le E\right)$
  if *converged* $=$ FALSE **then**
    for all $s \in \mathcal{S}$ **do**
      formDescs[s] $\leftarrow$ Algorithm3(s, H, C, V, D, *restVals*[s], *resoSelSol*, *hResoDepSols*[s])
    end for
    resoSelSol $\leftarrow$ ResoSelProb(*formDescs*)
  end if
  $j \leftarrow j+1$; *oldObj* $\leftarrow$ *newObj*
end while
return *resoSelSol*

Algorithm 3 Lower Level of Decomposition

Input: s, H, C, V, D, *sRestVals*, *resoSelSol*, *sHResoDepSols*
Output: *sFormDescs*

sFormDescs ← {}
for $h = 1, \ldots, H$ **do**
  if $h > 1$ **then**
    sHResoDepSols[h] ← `HResoDepProb`(s, D, *sRestVals*, *resoSelSol*, *sHResoDepSols*)
  end if
  for $t = |\mathcal{T}^s_{\mathrm{LT}}| + 1, \ldots, |\mathcal{T}|$ **do**
    formDesc ← `AddDescFullCount`(*sFormDescs*, h, t, *sHResoDepSols*[h], *sRestVals*)
    if *formDesc* = `NULL` **then** continue **end if**
    fullCount ← `GetResoCount`(*formDesc*)
    for $c = 1, \ldots, (C-1)$ **do**
      reducedCount ← $\lfloor$*fullCount* $\times\, c/C \rfloor$
      vResoDepSols ← {}
      for $v = 1, \ldots, V$ **do**
        vResoDepSols[v] ← `VResoDepProb`(t, *reducedCount*, *sRestVals*, *sHResoDepSols*[h], *vResoDepSols*)
        `AddDescReducedCount`(*sFormDescs*, h, t, c, v, *vResoDepSols*[v], *sRestVals*)
      end for
    end for
  end for
end for
return *sFormDescs*

$$\text{(b)}\ \forall u \in \mathcal{U}, \forall s \in \mathcal{S}, \forall t \in \mathcal{T}^s_{\mathrm{FT}}, \quad \sum_{f \in \mathcal{F}_{st}} A_{stuf}\, \rho_{stf} \le a_u,$$

$$\text{(c)}\ \forall w \in \mathcal{W}, \forall s \in \mathcal{S}, \forall t \in \mathcal{T}^s_{\mathrm{FT}}, \quad \sum_{f \in \mathcal{F}_{st}} E_{stwf}\, \rho_{stf} \le e_w,$$

$$\text{(d)}\ \forall s \in \mathcal{S}, \forall t \in \mathcal{T}^s_{\mathrm{FT}}, \quad \sum_{f \in \mathcal{F}_{st}} \rho_{stf} \le 1,$$

$$\text{(e)}\ \forall u \in \mathcal{U}, \quad a_u \le A_u, \quad \text{(f)} \sum_{u \in \mathcal{U}} a_u \le A_{\mathrm{TTL}},$$

$$\text{(g)}\ \forall w \in \mathcal{W}, \ e_w \le E_w, \ \text{(h)} \sum_{w \in \mathcal{W}} e_w \le E_{\mathrm{TTL}},$$

where $\mathcal{F}_{st}$ is the set of formations analyzed for FT interval t in scenario s, Δ_{stf} is the relief benefit of formation f in interval t of scenario s, ρ_{stf} is a binary variable indicating construction of formation f in interval t of scenario s, A_{stuf}, E_{stwf} are rating-specific MS resource requirements of formation f in interval t of scenario s, and a_u, e_w are an MS resource pre-selection that does not consider pre-positioning at depots. To avoid overestimation of relief benefit, at most one formation can be constructed in each FT interval of each scenario.

E. ALGORITHM 3: LOWER LEVEL OF DECOMPOSITION

Algorithm 3, which concerns only one scenario, starts with an empty dictionary of formation descriptions. For each iteration index $h = 1, \ldots, H$, the following steps are performed to produce formation descriptions, which are then recorded in the dictionary.

(I) If this is not iteration $h = 1$, then solve an `HResoDepProb` instance in view of locational dispersion D and the solutions of previous iterations' `HResoDepProb` instances.
- Unlike `HResoDepProb` instances in Algorithm 2, the instance here accepts the normal arguments to the function for the `HResoDepProb`, which are listed in Section III-C.
- This `HResoDepProb` instance must include constraints ensuring that, compared to each previous instance (for smaller h), the set of connection sites at which this instance ever deploys MS resources does not contain more than $(1 - D) \times 100\%$ of the same sites at which the previous instance ever deploys MS resources.
- Additionally, the pre-selection of MS resources must again be such that the quantity for a kind (i.e., MT or MB) and voltage rating does not differ by more than some fixed positive integer (e.g., 1) from its quantity in *resoSelSol*, which contains the pre-selection decided by step (IV) of the previous decomposition iteration.
- If this is iteration $h = 1$, then the remaining steps are to be performed using the solution of the `HResoDepProb` instance that Algorithm 2 solved for the scenario.

(II) For each FT interval t in the scenario, perform the following steps.
  (A) Execute `AddDescFullCount`, which assesses what connection sites have operational MS resources in the interval and, for the full formation observed, records a description containing the relief benefit and the quantity of each kind and voltage rating of MS resource.
  (B) If no connection sites have operational MS resources, then skip the remaining steps and proceed to (A) for the next FT interval in the scenario.
  (C) Execute `GetResoCount` to retrieve the total number of MS resources in the full formation.
  (D) For iteration indices $c = 1, \ldots, (C-1)$ and considering the value *fullCount* from (C), perform the following steps.
    (1) Calculate a reduced resource count *reducedCount* equal to $\lfloor$*fullCount* $\times\, c/C \rfloor$.
    (2) For each iteration index $v = 1, \ldots, V$, solve an instance of the interval-level resource deployment problem (abbreviated as `VResoDepProb`) that, subject to the following requirements, finds within the full formation of (A) the sub-formation that yields the greatest relief benefit.
      - While not exactly a variant of the TRP-MSR, the `VResoDepProb` accounts for optimal power flow. The objective function of the `VResoDepProb` is the sum of the costs of

real power generation and real load shed, as the cost of MS resource installation is neglected.

- Specifically, the VResoDepProb optimizes variants of the variables $\hat{a}^{st}_{l,\mathrm{O}}$, $\hat{a}^{st}_{l,\mathrm{D}}$, $\hat{e}^{st}_{x}$, $\hat{e}^{st}_{i,\mathrm{G}}$, and $\hat{e}^{st}_{i,\mathrm{L}}$, as well as variants of the variables for optimal power flow that are listed in Section III-A. However, unlike other subproblems, the VResoDepProb does not check whether an MS resource is installed for two consecutive intervals, as operational MS resources can only be chosen at connection sites that already have operational MS resources in the full formation of the FT interval. Moreover, only by one scenario s and one FT interval t are variables indexed.
- The sub-formation that the VResoDepProb instance produces cannot contain more than *reducedCount* MS resources.
- Each VResoDepProb instance after the one for $v = 1$ includes constraints requiring that the sub-formation found be different from the ones found by the previous instances (i.e., the instances for the same t, c but smaller v).

(3) For each sub-formation found by a VResoDepProb instance, execute AddDescReducedCount to record a description like the one recorded for the full formation.

F. DIAGRAMS OF INFORMATION FLOW

This subsection contains visualizations of the flow of information in algorithms 1, 2, and 3. The visualizations assume that every subroutine (indicated by a rectangle) has access to the problem parameters of the TRP-MSR instance, as well as to the inputs to Algorithm 1: J, E, H, C, V, and D. In this subsection, information is "passed" from one subroutine to a second subroutine if the first subroutine does not mutate the information in any manner before sending it to the second subroutine. The word "yield" is used in this subsection to refer to the creation of new information by a subroutine.

1) BODY OF ALGORITHM 1

Fig. 2 illustrates the flow of information in Algorithm 1. Algorithm 1 begins with an empty single-layer dictionary *restVals* indexed by scenario s. For each scenario s, a RestSeqProb instance is solved, yielding restoration-sequencing solution values (i.e., restoration values) that are saved in *restVals* as *restVals*[s]. The solution values saved in *restVals* are then passed, without mutation, through the body of Algorithm 1 to Algorithm 2, which in turn is executed to yield *resoSelSol*, solution values furnishing a pre-selection of MS resources. Lastly, *restVals* and *resoSelSol* are passed without mutation through the body of Algorithm 1 to the SolCompProb, which is solved to yield *heurSol*, a complete heuristic solution to the TRP-MSR instance.

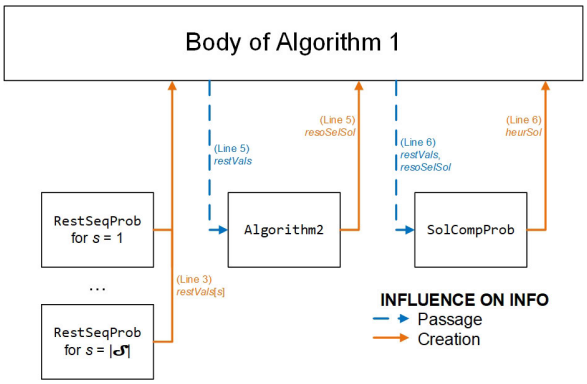

FIGURE 2. Flow of information in Algorithm 1.

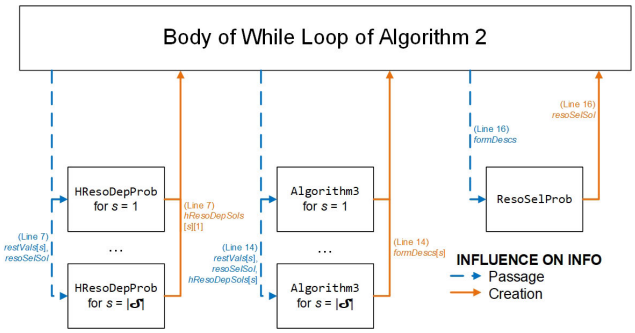

FIGURE 3. Flow of information in the while loop that starts on Line 3 of Algorithm 2.

2) WHILE LOOP OF ALGORITHM 2

Fig. 3 illustrates the flow of information in the while loop that starts on Line 3 of Algorithm 2. The while loop begins with an empty two-layer dictionary *hResoDepSols*, whose outer layer is indexed by scenario s and whose inner layer is indexed by horizon-level perturbation index h, and an empty single-layer dictionary *formDescs* indexed by scenario s. The loop also begins with predefined *restVals* and *resoSelSol*, except that the latter has value NULL in the first iteration of the loop. For each scenario s, an HResoDepProb instance is solved taking into account *restVals*[s] and *resoSelSol*. (The manner in which the HResoDepProb instance accounts for *resoSelSol* if it is not NULL is described in Section III-C.) When each HResoDepProb instance is solved, it yields solution values that are saved in *hResoDepSols* as *hResoDepSols*[s][1].

Then, the loop checks for convergence as described in Section III-C. If the loop considers there to be convergence, then the loop terminates. Otherwise, if convergence is not detected, then the body of the loop proceeds as follows. An instance of Algorithm 3 is executed for each scenario s, where *restVals*[s], *resoSelSol*, and *hResoDepSols*[s] are passed through the body of the loop to the instance of Algorithm 3, and the instance yields formation descriptions that are saved in *formDescs* as *formDescs*[s]. Lastly, *formDescs* is passed through the body of the loop to the ResoSelProb, which is solved to yield solution values on

MS resource pre-selection that replace the existing solution values in *resoSelSol*.

3) FOR LOOP OF ALGORITHM 3

Fig. 4 illustrates the flow of information in the for loop that starts on Line 2 of Algorithm 3. The for loop begins with predefined *sRestVals*, *resoSelSol*, and *sHResoDepSols*, where *sRestVals* denotes the solution values in *restVals*[s] and *sHResoDepSols* is the single-layer dictionary at *hResoDepSols*[s]. (It should be recalled that any instance of Algorithm 3 is for a specific scenario s.) Additionally, the for loop is over the horizon-level perturbation indices $h = 1, \ldots, H$. If h is greater than 1, then *sRestVals*, *resoSelSol*, and *sHResoDepSols* are passed through the body of the loop to the `HResoDepProb`, which is solved to yield solution values that are saved in *sHResoDepSols* as *sHResoDepSols*[h]. (If h is equal to 1, then an `HResoDepProb` instance is not solved because one is solved for $h = 1$ in Algorithm 2, and the solution values are already saved in *sHResoDepSols* as *sHResoDepSols*[1].) After the `HResoDepProb` is solved (if needed), a `VResoDepProb` instance is solved for each $t \in \{|\mathcal{T}^s_{\mathrm{LT}}| + 1, \ldots, |\mathcal{T}|\}$, each $c \in \{1, \ldots, (C-1)\}$, and $v = 1$.

Passed through the body of the loop to each of these `VResoDepProb` instances for $v = 1$ are *sRestVals*, *sHResoDepSols*[h], and *vResoDepSols*, where *vResoDepSols* is an empty dictionary indexed by interval-level perturbation index v. Each `VResoDepProb` instance for $v = 1$ is solved to yield solution values that are saved in *vResoDepSols*. Whenever any `VResoDepProb` instance is solved for $v = 1$, a `VResoDepProb` instance is then solved for $v = 2$ but the same t, c. Provided to the `VResoDepProb` instance for $v = 2$ are *sRestVals*, *sHResoDepSols*[h], and *vResoDepSols*, but *vResoDepSols* contains the solution values of the instance for $v = 1$. The manner in which a `VResoDepProb` instance accounts for the solution values of `VResoDepProb` instances for lower v but the same t, c is described in Section III-E. Like the instance for $v = 1$, the `VResoDepProb` instance for $v = 2$ is solved to yield solution values that are saved in *vResoDepSols*. As illustrated in Fig. 4, each `VResoDepProb` instance for v up to V likewise has *sRestVals*, *sHResoDepSols*[h], and *vResoDepSols* (containing the solution values of `VResoDepProb` instances for lower v but the same t, c) passed to it and is solved to yield solution values that are saved in *vResoDepSols*. Lastly, the body of the for loop in Algorithm 3 analyzes the solution values in *vResoDepSols* to create formation descriptions.

IV. EXPERIMENT SETUP

This section explains the setup of experiments conducted in two test systems: the IEEE 24-Bus System [59] and a synthetic Houston grid. While some aspects of the experiment setup are common to both systems, many aspects differ between them.

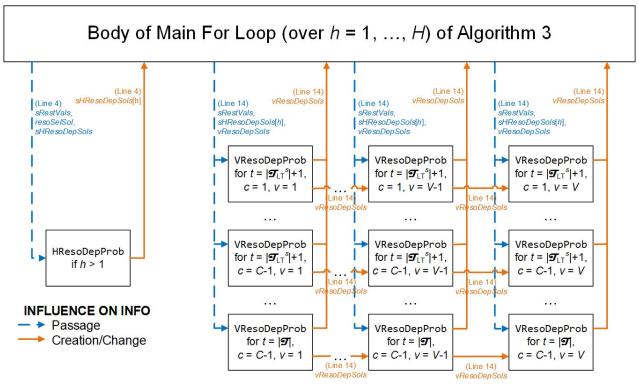

FIGURE 4. Flow of information in the for loop (over $h = 1, \ldots, H$) that starts on Line 2 of Algorithm 3.

A. SHARED SETUP

The optimization-model instances for numerical experiments are solved using Gurobi 9.1 [60] on a desktop computer with a 3.70-GHz, 8-core processor and 16 GB of RAM.

Experiments are conducted in both the IEEE 24-Bus System and a synthetic Houston grid. For experiments in both test systems, the time horizon consists of 18 24-hour intervals (i.e., days). MTs have capacities of 60 MVA if rated for generation step-up, 40 MVA if rated to augment branch transformers, or 20 MVA if rated for primary-distribution step-down. The staging costs are \$200,000 for an MT and \$100,000 for an MB. The installation costs are \$10,000 for an MT and \$5,000 for an MB. In both test systems, the experiments assume uniform generation cost and value of lost load of \$50/MWh and \$1,000/MWh, respectively, throughout the system.

B. SETUP IN IEEE 24-BUS SYSTEM

The experiments consider a one-line diagram that is taken from [61] and modified to reflect the setup, as shown in Fig. 5. The buses are divided into three partitions. As buses connected to each other by branch transformers are regarded as part of the same substation, there is no pair of buses that are connected by a branch transformer yet assigned to different partitions. Also, there are assumed to be four depots, and in Fig. 5 the substations reachable by each depot during the LT period have their bus numbers circled in a different color. Some bus numbers are circled in multiple colors, reflecting overlap between the depots' sets of substations. The buses above the branch transformers are rated at 230 kV while those below are rated at 138 kV. The voltage ratings for generation and primary distribution are assumed to be 25 kV and 12.47 kV, respectively.

For generating a scenario, each substation is independently disabled by flooding with the following probabilities: $\frac{1}{4}$ if the substation is in the top partition, $\frac{1}{3}$ if it is in the middle partition, or $\frac{1}{2}$ if it is in the bottom partition. If a substation is flooded, each of days 2 through 4 has an equal probability of being the first day of flooding at the substation, and each

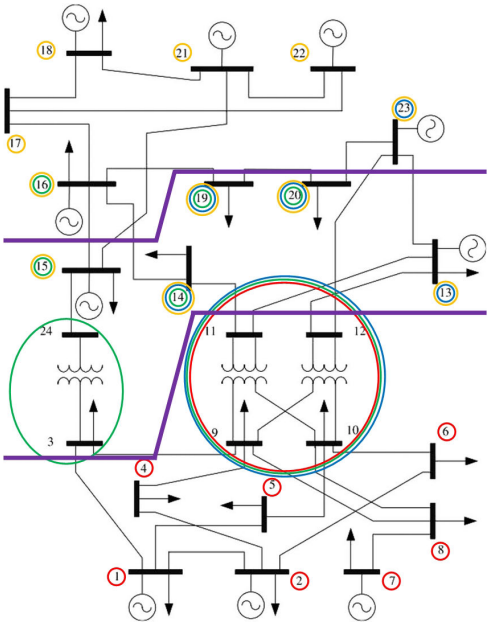

FIGURE 5. IEEE 24-Bus System with its partitions and its substations reachable by depots during the LT period.

of $\{2, 3, 4\}$ has an equal probability of being the number of days of flooding at the substation. Fifty scenarios are generated by the described method. Reinstatement of a permanent substation requires a number of labor units equal to 6 times the number of buses in the substation and can be completed within 6 days if performed at the maximum rate. In each FT interval, the total restoration labor system-wide is limited to 8 units. Without restrictions on voltage rating, the allowances for MTs and MBs are 5 and 10, respectively.

For each scenario count from 5 through 50 that is a multiple of 5, a subset of scenarios is drawn from the set of 50 scenarios. The scenarios for a count keep those of the preceding count and add five more scenarios from the 50. For each of these subsets of scenarios, the TRP-MSR instance is solved by four methods: serial execution of the heuristic, parallel execution of the heuristic, the extensive form (EF) for the full problem, and the EF with predetermined restoration. In the fourth method, the `RestSeqProb` is solved beforehand for each scenario separately (as in the heuristic) to determine the restoration values; the computation time then accounts only for solving the EF for the remaining problem, which has the restoration values fixed.

When the TRP-MSR instance for a scenario count is solved in EF—with or without predetermined restoration values—the time limit is set to 6 hours, and the optimality-gap tolerance is set to 2%. Similarly, when the TRP-MSR instance is solved by the heuristic, a time limit of 15 minutes is imposed on each `RestSeqProb` instance and on each `HResoDepProb` instance. Additionally, the default input setting to the heuristic has input values $J = 6, E = 0.01, H = 3, C = 5, V = 3, D = 0.50$. However, input settings changing one input at a time from its default value are also assessed. Thus, for each scenario count, what amounts to a one-factor-at-a-time (OFAT) experiment [62] is conducted. The following are the 11 different input values assessed: $E = 0.005, 0.025$; $H = 2, 4$; $C = 3, 7$; $V = 2, 4, 5$; and $D = 0.3333, 0.6667$. Including the default input setting, both serial and parallel execution of the heuristic occur for each of 12 input settings.

C. SETUP IN SYNTHETIC HOUSTON GRID

A synthetic Houston grid is produced by network reduction of the ACTIVSg2000 test system [63]. After usage of the electrical equivalent (EEQV) feature of Power System Simulator for Engineering (PSS®E) [64] on ACTIVSg2000, components in the EEQV result are relocated from buses below transmission level to transmission buses (i.e., rated at 115 kV or higher). Then, the buses below transmission level are removed. Ultimately, the synthetic Houston grid contains—centered on Houston—64 buses, 58 substations, 182 branches, 14.362 GW of total real generation capacity, and 8.193 GW of total real load demand.

Fig. 6 shows the synthetic Houston grid overlaid onto a geographical map of the Houston area. In the figure, each circle indicates a substation, and the color of the circle specifies the depot that can reach the substation during the LT period: blue for Depot 1, green for Depot 2, or orange for Depot 3. To reduce clutter, the substations have their numbers changed from what they were in ACTIVSg2000 to smaller numbers. Also depicted in the figure are transmission lines between substations; equivalent lines produced by the EEQV feature of PSS®E are colored in lime green, while actual 500-kV, 230-kV, and 115-kV lines are colored in magenta, cyan, and violet, respectively. The voltage ratings for generation and primary distribution are 20 kV and 34.5 kV, respectively. As the substations are (rather arbitrarily) assigned to depots by a k-means clustering approach, each substation can only be reached by one depot. In practice, the substations reachable by a depot will be specified to the TRP-MSR according to the expert knowledge of the power-system operators.

Reference [65] developed 25 equiprobable flood scenarios by geographical shifting of historical precipitation data from Hurricane Harvey. Of these 25 scenarios, for computational tractability, each TRP-MSR instance for the synthetic Houston grid considers only scenarios 12, 14, 16, 18, and 20; these scenarios are renumbered 1 through 5. These five scenarios are selected for their varied, though generally high, flood impact on the Houston area. Within a scenario, a substation is considered flooded whenever the flood height at the site exceeds 1 meter.

With the synthetic Houston grid and the five flood scenarios, solving in EF for the full problem is attempted for a default TRP-MSR instance. In the default instance, reinstatement of a permanent substation requires a number of labor units equal to 6 times the number of buses in the substation and can be completed within 6 days if performed

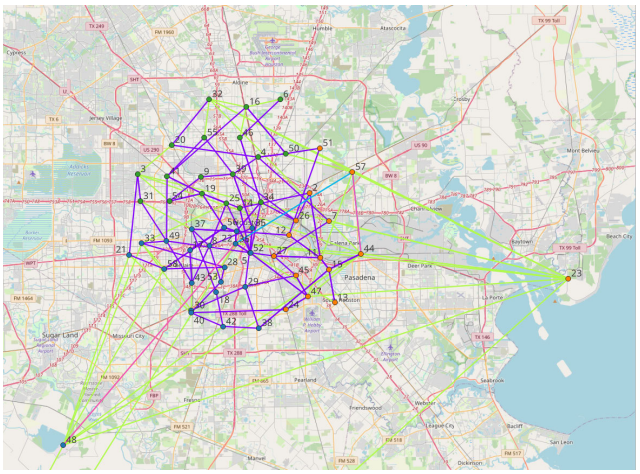

FIGURE 6. Synthetic Houston grid with its line voltage ratings, new substation numbers, and substations reachable by depots.

at the maximum rate. Moreover, the default instance limits the total restoration labor system-wide in each FT interval to 12 units. Without restrictions on voltage rating, the allowances for MTs and MBs are 4 and 8, respectively.

Even after 156 hours (i.e., 6.5 days) of solution time, the EF has still only reached an optimality gap of 6.74%. Following the interruption of the EF, a tuning investigation is conducted in which the default TRP-MSR instance is solved by parallel execution of the heuristic under a variety of input settings. Ultimately, relative to the default input setting described in Section IV-B, it is determined that the non-default input values of $C = 7, V = 5, D = 0.75$ accomplish a reasonable balance of total computation time—8.111 hours—and optimality gap—6.28% relative to the EF's best lower bound at interruption. (In total across the depots, of the eight MBs staged, five are rated at 115 kV, two at 230 kV, and one at 500 kV. Of the four MTs staged, all are rated for primary-distribution step-down: three with a high-side rating of 115 kV and one with a high-side rating of 230 kV.) Therefore, all TRP-MSR instances after the default one are solved by parallel execution of the heuristic with these selected input values. An assumption is made that, even if these input values are not the best for a different TRP-MSR instance, they will still perform adequately for that instance.

Naturally, concerns may arise about the adequacy of the prospective sample of scenarios—the five scenarios 12, 14, 16, 18, and 20, which collectively may be called Sample A—for representing the scenario distribution in the synthetic Houston grid. To allay such concerns, the default TRP-MSR instance is solved again by parallel execution of the heuristic with the selected input values but with larger samples (i.e., subsets) of the full set of 25 flood scenarios developed in [65]. Instead of considering every other scenario as Sample A does, Sample B consists of all ten scenarios in the range 11 through 20. Sample C consists of the 18 scenarios in the range 4 through 21, for scenarios outside this range do not flood any substation contained in the synthetic Houston grid. Sample D is the full set of 25 scenarios.

If the TRP-MSR instance is solved for samples A through D, then the objective values in $MM are 441.468, 440.512, 443.719, and 368.497, respectively. The high similarity of the first three objective values suggests that Sample A may be acceptable for representing the scenario distribution in the synthetic Houston grid. That the fourth objective value is much lower than the first three can be attributed to the absence of load shed in the seven scenarios without flood damage. The first-stage decisions are also sufficiently similar: all four samples result in staging at least four MBs rated at 115 kV, at least one rated at 230 kV, and exactly two rated at 500 kV. Moreover, all four samples result in staging four MTs whose high-side ratings may differ but whose low-side rating is 34.5 kV, which is for primary distribution.

With the selected input values, a 2^3 full factorial experiment [62] is conducted in the synthetic Houston grid. Three factors, each having two levels, are varied in the experiment. Factor A is the maximum total restoration labor system-wide $\overline{Y}^{st}$ in each FT interval and has levels of 6 units (designated as $-$) and 18 units ($+$). Factor B is the maximum restoration labor at a substation $\overline{Y}_n^{st}$ in each FT interval and has levels of 0.5 units per bus ($-$) at the substation and 1.5 units per bus ($+$). Factor C is the MT allowance E_{TTL}—twice which is the MB allowance A_{TTL}—and has levels of 0 ($-$) and 4 ($+$). For each of the eight treatment combinations, two replicates are run to assess the influence of random, experimental error—such as from variation in the objective value that a subproblem achieves by its time limit—on response values.

V. EXPERIMENT RESULTS

This section discusses results of experiments in both the IEEE 24-Bus System and the synthetic Houston grid. Since experiments in the IEEE 24-Bus System are chiefly intended to demonstrate the performance of the heuristic, Section V-A describes in general terms the results of experiments in the IEEE 24-Bus System while Section V-B provides a stability test. Nevertheless, as the IEEE 24-Bus System is simpler than the synthetic Houston grid, it is with the IEEE 24-Bus System that an example of the formations concept is furnished in Section V-C. Then, Section V-D summarizes results of experiments in the synthetic Houston grid, while Section V-E examines in detail the results for Replicate 1 of treatment combinations $(-, -, -)$ and $(+, +, +)$.

A. IEEE 24-BUS SYSTEM RESULTS

Fig. 7 shows the computation times for the four methods of solving the TRP-MSR instances; for either EF, reaching the time limit is reflected by a time of 6 hours. Fig. 8 shows the optimality gaps calculated relative to the best lower bound that the branch-and-bound algorithm of the EF for the full problem has found by the time of termination, due to reaching either the optimality-gap tolerance or the time limit. In both figures, the dots of the swarm plot correspond to executions of the heuristic under different input settings.

Parallel execution of the heuristic tends to achieve the shortest computation times, followed by serial execution of

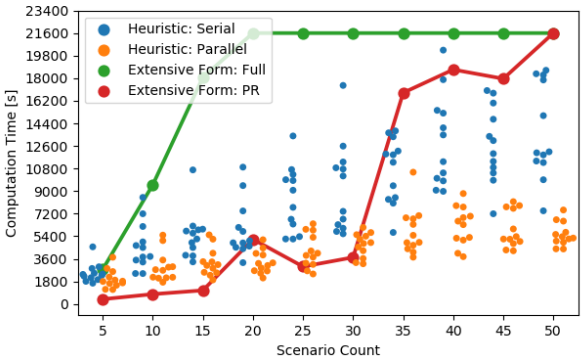

FIGURE 7. Computation time v. scenario count for serial execution of the heuristic, parallel execution of the heuristic, the extensive form for the full problem, and the extensive form with predetermined restoration.

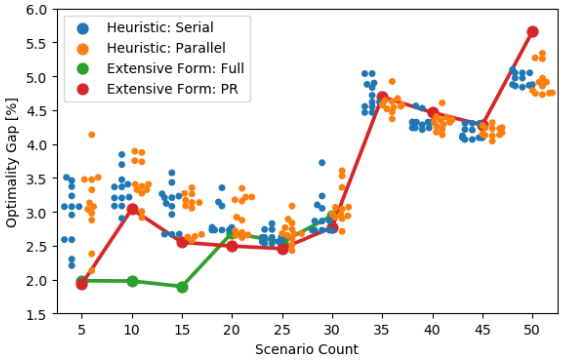

FIGURE 8. Optimality gap v. scenario count for serial execution of the heuristic, parallel execution of the heuristic, the extensive form for the full problem, and the extensive form with predetermined restoration.

the heuristic, the EF with predetermined restoration, and lastly the EF for the full problem. The optimality gap achieved by the heuristic is usually between 2.5% and 3.5%. For scenario counts of 20, 25, and 30, the EF for the full problem times out before reaching the 2% optimality gap. For scenario counts of 35, 40, and 50, the EF for the full problem times out before finding an integer-feasible solution, so the EF for the full problem has no optimality gap displayed. (The EF for the full problem does find an integer-feasible solution for the scenario count of 45, but the solution's optimality gap is a staggering 21.8995%.) In contrast, even for 50 scenarios, parallel execution of the heuristic completes within 2 hours in most cases. Moreover, because the EF for the full problem times out for scenario counts of 35 and above before it can find a tight lower bound, the heuristic's optimality gaps calculated for these relatively large counts are also not as low as for smaller counts.

Solution of the TRP-MSR instances by the EF with predetermined restoration affords insights not possible solely from solution by the EF for the full problem. For example, it is observed that the EF with predetermined restoration does offer computational expedience without necessarily sacrificing solution quality. For scenario counts of 20, 25, and 30, the EF for the full problem achieves optimality gaps of less than 3% by the time limit of 6 hours, yet the EF with predetermined restoration achieves even lower optimality

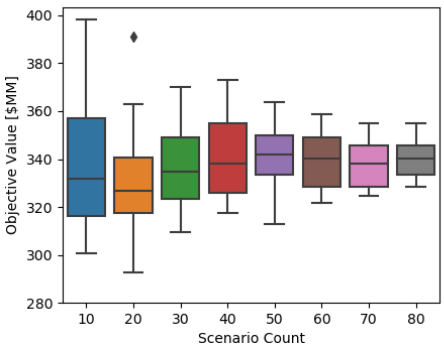

FIGURE 9. Box plot from stability test of the TRP-MSR in the IEEE 24-Bus system.

gaps while finishing in no more than 1.5 hours. Likewise, it is in turn confirmed that the heuristic, compared to the EF with predetermined restoration, offers computational expedience without necessarily sacrificing solution quality. For scenario counts of 40, 45, and 50, the EF with predetermined restoration requires at least 5 hours to finish, yet parallel execution of the heuristic achieves lower optimality gaps while finishing within 2 hours in most cases.

For every scenario count, execution of the heuristic with each input setting achieves the convergence tolerance in no more than two complete iterations. Nevertheless, computation time and the number of iterations tend to decrease as the convergence tolerance E increases. Computation time usually increases with horizon-level perturbations H while the number of iterations does not. Also, the optimality gap tends to decrease with horizon-level perturbations H and interval-level perturbations V.

B. STABILITY TEST

A stability test is conducted to assess whether the scenario count of 50—the greatest scenario count of any TRP-MSR instance in the IEEE 24-Bus System—is adequate for representing the scenario distribution in the IEEE 24-Bus System. The thought is that if the scenario count of 50 is adequate, then the computation speed and solution quality of the parallel heuristic need not be confirmed for higher scenario counts.

By the same scenario-generation method described in Section IV-B, 16 distinct sets of 80 scenarios are generated in the IEEE 24-Bus System. Then, the following steps are executed for each set of 80 scenarios.

(I) For each scenario count from 10 through 80 that is a multiple of 10, draw a subset of scenarios from the set of 80. The scenarios for a count keep those of the preceding count and add ten more scenarios from the 80.

(II) For each of these subsets of scenarios, solve the TRP-MSR instance by parallel execution of the heuristic under the default input setting.

Fig. 9 provides a box plot of the objective values yielded by these steps. It is observed that, in accordance with the concept of the optimizer's curse, the median objective value

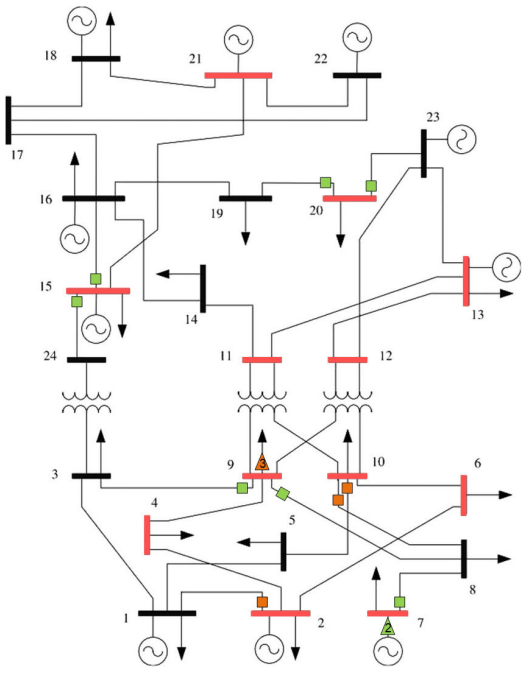

FIGURE 10. Full formation (both orange and green) on Day 8 of the `HResoDepProb` solution for $j = 1$, $h = 1$, and Scenario 2, as well as the sub-formation (green only) in the `VResoDepProb` solution for $j = 1$, $h = 1$, $c = 3$, $v = 1$, Scenario 2, and Day 8.

tends to be lower (i.e., more optimistic) for smaller scenario counts than for larger scenario counts. Nevertheless, the median objective value \$341.919MM for the scenario count of 50 is approximately as high (i.e., realistic) as the median objective value \$340.281MM for the scenario count of 80. Additionally, the interquartile range (IQR) \$16.424MM for the scenario count of 50 is almost as narrow as the IQR \$12.138MM for the scenario count of 80; that is, the scenario count of 80 does not substantially further limit variation in the objective values of TRP-MSR instances. The IQR \$12.138MM is merely 3.5670% of \$340.281MM. Thus, it can be concluded that the scenario count of 50 is already quite adequate for representing the scenario distribution in the IEEE 24-Bus System.

C. EXAMPLE OF FORMATIONS CONCEPT

Within the complete solution to the five-scenario TRP-MSR instance in the IEEE 24-Bus System, one of the intervals with the most operational MS resources is Day 8 of Scenario 2. As may be expected, the prevalence of operational MS resources on Day 8 is heralded even by solutions to instances of `HResoDepProb` and `VResoDepProb`, subproblems of the heuristic used to solve the TRP-MSR instance. Illustrated in Fig. 10 are the operational MS resources on Day 8 of the solution to the `HResoDepProb` instance for $j = 1$, $h = 1$, and Scenario 2. Also illustrated in the figure are the operational MS resources in the solution to the `VResoDepProb` instance for $j = 1$, $h = 1$, $c = 3$, $v = 1$, Scenario 2, and Day 8.

In Fig. 10, an MB at the origin or destination of a line is marked with a square. MTs substituting for generation step-up at a bus are marked with a triangle that points toward the busbar and contains a number indicating the quantity of substituting MTs. MTs substituting for primary-distribution step-down at a bus are marked with a triangle that points away from the busbar and again indicates the quantity of MTs. Day 8 of the `HResoDepProb` solution does not involve MTs substituting for branch transformers, nor does the `VResoDepProb` solution. The symbols for the operational MS resources of the `VResoDepProb` solution are colored green. The symbols for the MS resources operational only on Day 8 of the `HResoDepProb` solution, not operational in the `VResoDepProb` solution, are colored orange. (It happens that there is no connection site at which the `VResoDepProb` solution has a smaller—but nonzero—quantity of operational MS resources than does Day 8 of the `HResoDepProb` solution.) The MS resources colored green can be considered a sub-formation of the full formation, which is given by all MS resources—colored orange or green—in the figure. Buses whose connection sites are disabled by flooding earlier in Scenario 2 have their busbars colored red.

Within the solution to the `RestSeqProb` instance for Scenario 2, the sum of the costs on Day 8 of real power generation and load shed is \$45.604MM. Within the solution to the `HResoDepProb` instance for $j = 1$, $h = 1$, and Scenario 2, the sum of the costs on Day 8 of real power generation and load shed is \$36.526MM, so the relief benefit of the full formation observed for Day 8 of the `HResoDepProb` solution is \$45.604MM − \$36.526MM = \$9.078MM. The MS resource requirements of the full formation are two 138/25-kV MTs, three 138/12.47-kV MTs, six 138-kV MBs, and four 230-kV MBs. Likewise, within the solution to the `VResoDepProb` instance for $j = 1$, $h = 1$, $c = 3$, $v = 1$, Scenario 2, and Day 8, the total cost (i.e., sum of the costs of real power generation and load shed) is \$37.894MM, so the relief benefit of the sub-formation observed in the solution is \$7.710MM. The MS resource requirements of the sub-formation observed in the `VResoDepProb` solution are two 138/25-kV MTs, three 138-kV MBs, and four 230-kV MBs. As the *fullCount* of the full formation is 15, the *reducedCount* of the sub-formation should be $\lfloor fullCount \times c/C \rfloor = \lfloor 15 \times 3/5 \rfloor = \lfloor 9 \rfloor = 9$. Indeed, the sub-formation observed involves exactly nine MS resources, though it could have involved fewer, just not more.

Table 1 reports the findings from a similar analysis of the solutions to the `VResoDepProb` instances for $j = 1$, $h = 1$, $v = 1$, Scenario 2, and Day 8 but all possible values of c. The full formation is denoted by a value of c equal to C, which is 5. The sub-formation observed in the solution for $c = 1$ has an MB at the origin of Line 7-8 and two MTs at the generation step-up connection of Bus 7. The sub-formation observed in the solution for $c = 2$ has an MB at each of the origins of lines 7-8, 15-16, 15-24, and 20-23 and at the destination of Line 19-20, as well as one MT at the generation step-up connection of Bus 7. The sub-formation

TABLE 1. Characteristics of sub-formations for Day 8 of Scenario 2.

Value of c	Value of *reducedCount*	Actual Number of Resources	Total Cost ($MM)	Relief Benefit ($MM)	Marginal Relief Benefit ($MM)
1	3	3	43.780	1.824	1.824
2	6	6	40.881	4.723	2.899
3	9	9	37.894	7.710	2.987
4	12	12	36.570	9.034	1.324
5	15	15	36.526	9.078	0.044

observed in the solution for $c = 4$ has an MB at each of the origins of lines 7-8, 15-16, 15-24, and 20-23 and at each of the destinations of lines 3-9, 8-9, and 19-20, as well as two MTs at the generation step-up connection of Bus 7 and three MTs at the primary-distribution step-down connection of Bus 9. From Table 1, it is seen that the marginal relief benefit (i.e., the increase in relief benefit from increasing c by 1) is actually increasing until $c = 3$, beyond which the marginal relief benefit is decreasing.

D. SYNTHETIC HOUSTON GRID RESULTS: SUMMARY

Table 2 provides response values (i.e., objective values achieved by parallel execution of the heuristic) gathered for the treatment combinations of the 2^3 factorial experiment conducted in the synthetic Houston grid. Table 3 contains findings from the statistical analysis of the response values.

The findings in Table 3 should be considered in light of the fact that they describe the cubical region enclosed by the low (−) and high (+) levels of the three factors A, B, and C. (Nevertheless, experiment runs considering intermediate values for the factors have generally upheld the findings.) With this in mind, it is seen in the table that the main effects A, B, and C all have negative estimated values of substantial magnitude, which indicate that an increase in any of $\overline{Y}^{st}$, $\overline{Y}^{st}_n$, E_{TTL} generally leads to a decrease in the objective value (i.e., benefits recovery of the transmission network). The values in the "Percent of Default Obj." column are calculated relative to the objective value of the default TRP-MSR instance. Interactions AB and BC also have notable estimated values.

The negative estimated value for AB reflects the tendency that increasing $\overline{Y}^{st}_n$ brings greater benefit to recovery when $\overline{Y}^{st}$ is high. This tendency holds intuitive appeal since with more labor system-wide, the power-system operators can better capitalize on the ability to restore individual substations faster. Likewise, the negative estimated value for AB additionally reflects that increasing $\overline{Y}^{st}$ brings greater benefit to recovery when $\overline{Y}^{st}_n$ is high.

However, it is more interesting that BC has a positive estimated value, evincing the tendency that increasing E_{TTL}, twice which is A_{TTL}, brings greater benefit to recovery when $\overline{Y}^{st}_n$ is low rather than high. When critical substations require longer to restore, the ability of MS resources to temporarily substitute for connections proves especially valuable. Likewise, the positive estimated value for BC evinces that increasing $\overline{Y}^{st}_n$ brings greater benefit to recovery when E_{TTL} is low.

TABLE 2. Response values of factorial experiment for Houston grid.

CODED FACTORS			OBJECTIVE VALUE ($MM)	
A ($\overline{Y}^{st}$)	B ($\overline{Y}^{st}_n$)	C (E_{TTL})	Replicate 1	Replicate 2
+	+	+	371.871	371.871
+	+	-	393.448	393.448
+	-	+	545.233	545.818
+	-	-	592.766	592.766
-	+	+	425.513	425.513
-	+	-	449.103	449.103
-	-	+	547.034	543.021
-	-	-	592.766	592.766

TABLE 3. Main effects and interactions of factorial experiment.

Effect	Estimated Value ($MM)	Percent of Default Obj.	Mean Squares	P-Value
A	-27.1999	-6.1612	2959.336	0.000000
B	-159.0378	-36.0248	101172.140	0.000000
C	-35.0367	-7.9364	4910.292	0.000000
AB	-27.4489	-6.2176	3013.760	0.000000
AC	0.6278	0.1422	1.577	0.250620
BC	12.4528	2.8208	620.291	0.000000
ABC	0.3788	0.0858	0.574	0.476236

TABLE 4. MS resources pre-selected by first replicates.

CODED FACTORS			PRE-SELECTED MOBILE RESOURCES	
A ($\overline{Y}^{st}$)	B ($\overline{Y}^{st}_n$)	C (E_{TTL})	MTs (Staged at Depots)	MBs (Staged at Depots)
+	+	+	Four 500/34.5-kV (at Z1)	Four 115-kV (two at Z1, two at Z2), two 230-kV (at Z2), two 500-kV (at Z1)
+	-	+	Four 115/34.5-kV (at Z3)	Five 115-kV (four at Z1, one at Z3), two 230-kV (at Z2), one 500-kV (at Z1)
-	+	+	Four 115/34.5-kV (at Z2)	Five 115-kV (three at Z1, two at Z2), one 230-kV (at Z2), two 500-kV (at Z1)
-	-	+	Four 115/34.5-kV (at Z3)	Five 115-kV (three at Z1, two at Z3), one 230-kV (at Z2), two 500-kV (at Z1)

For the 2^3 factorial experiment, the sum of squares due to error has eight degrees of freedom. Assuming objective values are in $MM, the mean square error has a calculated value of 1.027718. Additionally, each effect has a sum of squares with one degree of freedom. Determined by an F-test approach in [62] that compares the mean squares of an effect to the mean square error, the p-value of each effect in Table 3 describes the significance level at which one can reject a null hypothesis: that the effect has no influence on the objective value. From Table 3, it is seen that interactions AC and ABC have p-values greater than 0.05, suggesting that the estimated values of these two interactions may simply be due to random error.

For each treatment combination with the MT allowance of 4, tables 4 and 5 detail how the MS resources are pre-selected and staged in replicates 1 and 2, respectively. A depot is designated with "Z" followed by the index of

TABLE 5. MS resources pre-selected by second replicates.

CODED FACTORS			PRE-SELECTED MOBILE RESOURCES	
A ($\overline{Y}^{\mathrm{SI}}$)	B ($\overline{Y}_n^{\mathrm{SI}}$)	C (E_{TTL})	MTs (Staged at Depots)	MBs (Staged at Depots)
+	+	+	Four 500/34.5-kV (at Z1)	Four 115-kV (two at Z1, two at Z2), two 230-kV (at Z2), two 500-kV (at Z1)
+	-	+	Four 115/34.5-kV **(one at Z1, three at Z3)**	**Seven 115-kV (five at Z1, one at Z2, one at Z3)**, one 500-kV (at Z1)
-	+	+	Four 115/34.5-kV (at Z2)	Five 115-kV (three at Z1, two at Z2), one 230-kV (at Z2), two 500-kV (at Z1)
-	-	+	Four 115/34.5-kV (at Z3)	**Eight 115-kV (five at Z1, two at Z2, one at Z3)**

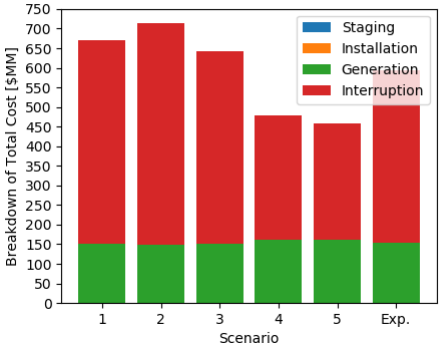

FIGURE 11. Breakdown of total cost in Replicate 1 of (−, −, −).

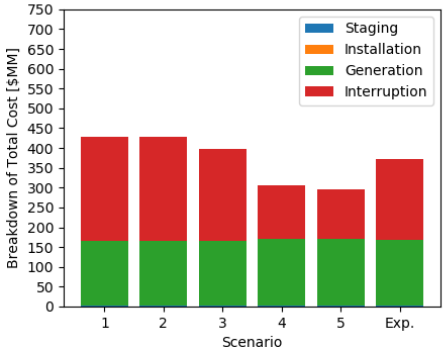

FIGURE 12. Breakdown of total cost in Replicate 1 of (+, +, +).

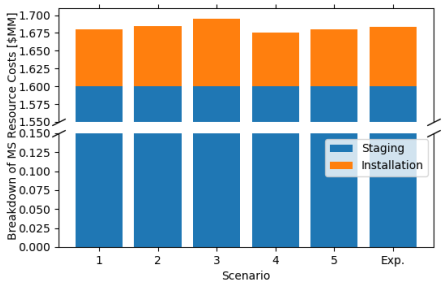

FIGURE 13. Breakdown of MS resource costs in Replicate 1 of (+, +, +).

the depot (e.g., "Z1" designates Depot 1). While the two replicates yield mostly identical pre-selection and staging of MS resources, Replicate 2 of treatment combination (+, −, +) stages the four pre-selected 115/34.5-kV MTs differently than does Replicate 1. Moreover, in place of the two 230-kV MBs pre-selected in Replicate 1 of treatment combination (+, −, +), two more 115-kV MBs are pre-selected in Replicate 2. Likewise, while Replicate 1 of (−, −, +) pre-selects three MBs to have voltage ratings other than 115 kV (one at 230 kV and two at 500 kV), Replicate 2 of (−, −, +) pre-selects all eight MBs to be rated at 115 kV. Apparently, since 115 kV is such a ubiquitous voltage rating in the synthetic Houston grid, it is not difficult to find applications for 115-kV MBs just as worthwhile as applications that 230-kV and 500-kV MBs would have.

E. SYNTHETIC HOUSTON GRID RESULTS: DETAILS

This subsection examines in detail the results of Replicate 1 of treatment combinations (−, −, −) and (+, +, +).

Fig. 11 illustrates the breakdown of the total cost in each scenario—and in expectation—of Replicate 1 of (−, −, −). Clearly, since the staging cost is incurred in the first stage, all five scenarios share the same staging cost. Nevertheless, the staging cost is so negligible compared to other costs that it hardly appears in the figure. The installation cost is similarly negligible and thus not visible. In contrast, the generation cost is substantial in all scenarios, even compared to the load-interruption cost (i.e., the cost of load shed). As the parametrized value of lost load is 20 times greater than the parametrized generation cost per unit energy, the reader may initially be surprised that the load-interruption cost does not utterly dominate the generation cost, at least until the reader notices that the generation cost is approximately the same in all scenarios. Since load that is supplied by generation is not shed, the lack of variation in the generation cost reflects that while the portion of load energy that is unserved over the horizon does not constitute even one-fifth in any scenario, the extent to which the value of lost load exceeds the generation cost per unit energy magnifies the load-interruption cost.

Fig. 12 illustrates the breakdown of the total cost in each scenario—and in expectation—of Replicate 1 of (+, +, +). The generation cost is slightly higher than in Fig. 11, but the load-interruption cost is appreciably lower. These two general changes in the costs can be attributed to how (+, +, +), with its MS resources and expedited restoration of permanent substations, more rapidly reconnects load to the transmission network than does (−, −, −).

Fig. 13 illustrates the breakdown of MS resource costs in each scenario—and in expectation—of Replicate 1 of (+, +, +). As a first-stage cost, the same staging cost of approximately $1.6MM is seen in all five scenarios. Because each scenario has approximately the same installation cost of $75,000, no scenario appears to find especially inadequate usage of the MS resources. More generally, it should also be noticed how, as long as the staging cost of MS resources does not pose too heavy a financial burden, $1.6MM utterly

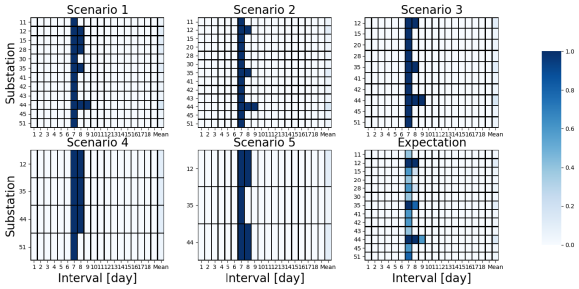

FIGURE 14. Substation flooding, irrespective of factor levels.

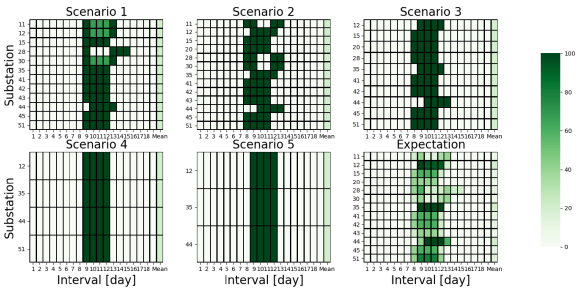

FIGURE 15. Proportion of maximum restoration labor rate at substations in Replicate 1 of (+, +, +).

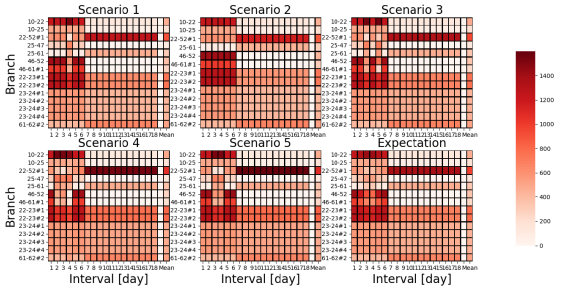

FIGURE 16. MVA loading of branches in Replicate 1 of (−, −, −).

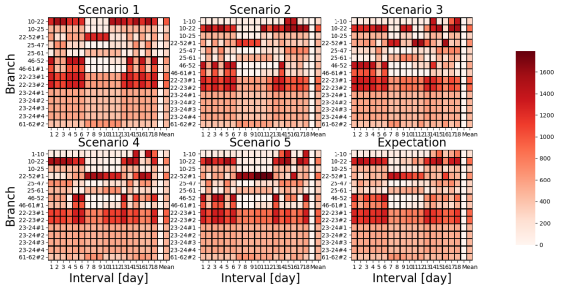

FIGURE 17. MVA loading of branches in Replicate 1 of (+, +, +).

dominating $75,000 bespeaks the practicality of deploying MS resources flexibly over an extended restoration period.

Fig. 14 indicates which substations are flooded on each day of each scenario, irrespective of the levels of the three factors. Substations 12, 35, and 44 are flooded in all five scenarios. It should be noted that substations 1-21, 23-43, 45-56, and 58 each contain a single bus: buses 1-21, 25-45, 49-60, and 64, respectively. Substation 22 contains buses 22-24. Substation 44 contains buses 46-48; consequently, these buses are flooded in all five scenarios, as are buses 12 and 37. Substation 57 contains buses 61-63. In each scenario, flooding at a substation starts on Day 7 and lasts one to three days. Scenarios 1, 2, and 3 affect many more substations than do scenarios 4 and 5.

Fig. 15 depicts the proportion of the maximum restoration labor rate $\overline{Y}_n^{st}$ that occurs at each substation on each day of each scenario. Within a scenario, restoration labor is permitted only during the FT period, so the first day on which any restoration labor is observed effectively marks the start of the FT period. It is seen that, while restoration of a substation commonly proceeds at maximum speed until reinstatement, sometimes substations have their restoration efforts interleaved so that they are reinstated at roughly the same time. A figure like Fig. 15 is not provided for (−, −, −) because the low level of 0.5 units per bus for Factor B ($\overline{Y}_n^{st}$) prevents any substation from being reinstated within the horizon. Reinstatement of a substation requires 6 units per bus, as mentioned in Section IV-C, yet no scenario has an FT period longer than 12 days.

Fig. 16 depicts the MVA loading of branches in Replicate 1 of (−, −, −). Branches are identified by their origin and destination buses (e.g., Line 22-52 #1 refers to the first line between buses 22 and 52 while Line 10-22 refers to the only line between buses 10 and 22). Substation 44, which contains buses 46-48, is flooded starting on Day 7 of each scenario. As a result, flow is inhibited in lines 25-47, 46-52, and 46-61 #1. In turn, less of the real power generated at Bus 10 is routed through Line 10-25 to Bus 25, and less of the real power generated at Bus 22 is routed through Line 10-22 to Bus 10. Fig. 17 depicts the MVA loading of branches in Replicate 1 of (+, +, +). The reinstatement of Substation 44 by the end of Day 12 or Day 13 of each scenario permits heavy loading to resume in lines 46-52 and 46-61 #1 starting on Day 13 or Day 14. In a manner explained later, MBs improve the connectivity of the network even before substations are reinstated, so that heavy loading resumes in lines 10-22 and 10-25 on Day 9 of Scenario 3 and on Day 11 of scenarios 1 and 2.

Fig. 18 depicts the real generation in MW at buses in Replicate 1 of (−, −, −). Buses 10 and 22 are observed to generate less real power once substations start to be flooded. However, buses 10 and 22 are at substations 10 and 22, respectively, neither of which is flooded in any of the five scenarios. The flooding of substations whose buses host load, or of substations connecting such substations, is what causes buses 10 and 22 to start generating less real power. Fig. 19 depicts the real generation in MW at buses in Replicate 1 of (+, +, +). Buses 10 and 22 are observed to resume generating large amounts of real power not long after substations start to be flooded. It is explained later that,

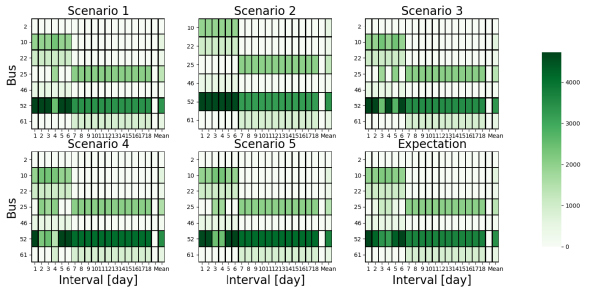

FIGURE 18. Real generation in MW at buses in Replicate 1 of (−, −, −).

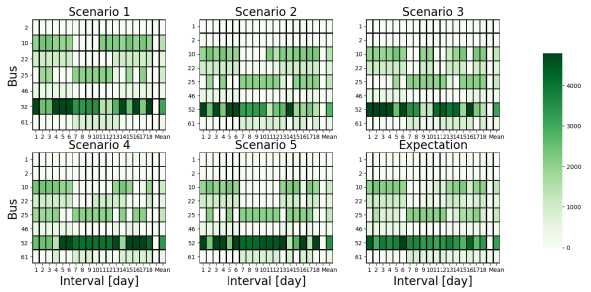

FIGURE 19. Real generation in MW at buses in Replicate 1 of (+, +, +).

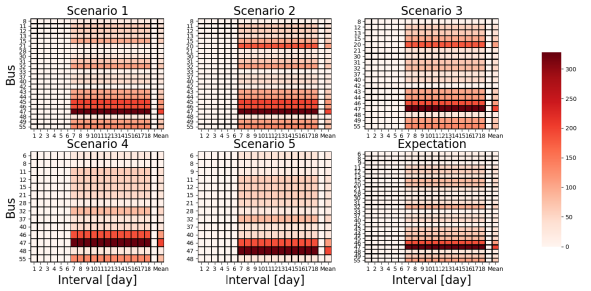

FIGURE 20. Real load shed in MW at buses in Replicate 1 of (−, −, −).

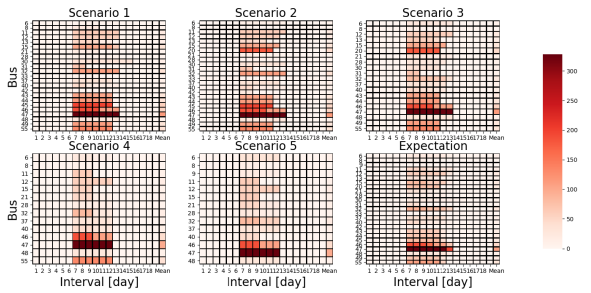

FIGURE 21. Real load shed in MW at buses in Replicate 1 of (+, +, +).

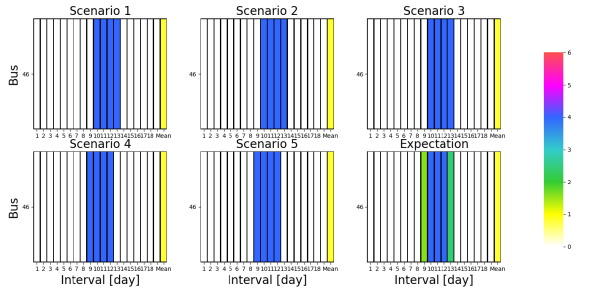

FIGURE 22. MTs deployed for primary distribution at substations in Replicate 1 of (+, +, +).

besides improved network connectivity from reinstatement of substations and deployment of MBs, MTs substitute for the disabled primary-distribution step-down connection through which load at Bus 46 is connected to the transmission network.

Fig. 20 depicts the real load shed in MW at buses in Replicate 1 of (−, −, −). Substation 44, which contains buses 46-48, is flooded in all five scenarios; consequently, load shed occurs especially at buses 46 and 47, which host load demands of 186.925 MW and 327.664 MW, respectively. In scenarios 1 through 3, buses 43, 44, 49, and 55 experience substantial load shed. These four buses are at substations 41, 42, 45, and 51, respectively, which are indeed flooded in scenarios 1 through 3. Similarly, in scenarios 2 and 3, Bus 20 experiences load shed due to flooding at Substation 20, which contains Bus 20. In scenarios 1 and 2, Bus 45 experiences load shed due to flooding at Substation 43, which contains Bus 45. Thus, it appears that most load shed occurs at buses directly in flooded substations. Fig. 21 depicts the real load shed in MW at buses in Replicate 1 of (+, +, +). At the buses with load shed, it is seen to disappear before the end of the horizon. Nevertheless, unlike the resumption of generation at buses 10 and 22 described previously, the disappearance of load shed mostly does not occur until Day 13 or Day 14 and is largely due to the reinstatement of substations, not the installation of MS resources.

Fig. 22 depicts the deployment of MTs in Replicate 1 of (+, +, +). The allowance of MTs is 4, and each MT has a capacity of 20 MVA because, as indicated in Table 4, all four pre-selected MTs are rated for primary-distribution step-down. Thus, the four MTs furnish a total capacity of 80 MVA. This total capacity is fully utilized when for four days starting on Day 9 or Day 10 of each scenario, the four MTs are deployed at Bus 46, which hosts a load demand of 186.925 MW. It should be noted that, since the first day of deployment is spent on installation, the MTs are operational at Bus 46 only starting on Day 10 or Day 11. The entry of the MTs into operation is reflected in Fig. 21, which shows three days of reduced load shed at Bus 46 in each scenario.

Fig. 23 and 24 depict the deployment of MBs at the origins and destinations, respectively, of lines in Replicate 1 of (+, +, +). The voltage ratings for which MBs are pre-selected are detailed in Table 4. Since in every scenario MTs are deployed to substitute for the primary-distribution step-down connection at Bus 46, the deployment of MBs is partly intended to reconnect lines to Bus 46. In scenarios 1 and 3, one connection with an MB deployed is the origin of Line 46-52. As seen in Fig. 19, Bus 52 generates large

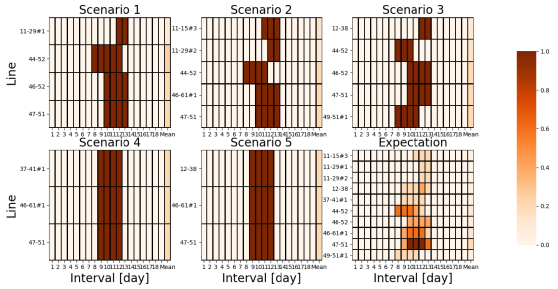

FIGURE 23. MBs deployed at origins of lines in Replicate 1 of (+, +, +).

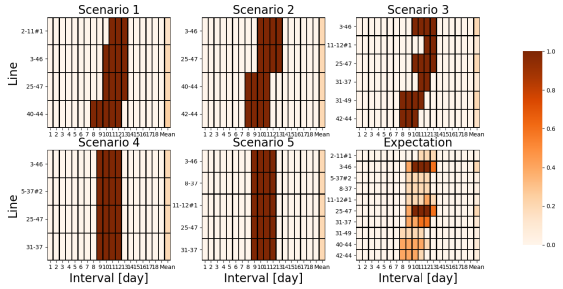

FIGURE 24. MBs deployed at destinations of lines in Replicate 1 of (+, +, +).

amounts of real power. With an MB reconnecting Line 46-52 to Bus 46, real power generated at Bus 52 can be supplied to load at Bus 46 through Line 46-52 and the MTs deployed at Bus 46. The other connections at Bus 46 with MBs deployed are the origin of Line 46-61 #1 in scenarios 2, 4, and 5 and the destination of Line 3-46 in all scenarios. Although Bus 61 generates some real power, Bus 3 does not.

Likewise, instead of directly linking generation to load, some connections with MBs deployed bring less direct benefits to the connectivity of the transmission network. Since an MB is deployed at the origin of Line 44-52 in scenarios 1 through 3, the MB deployed at the destination of Line 40-44 in scenarios 1 and 2 and the one deployed at the destination of Line 42-44 in scenarios 2 and 3 indirectly link the generation capacity at Bus 52 to buses 40 and 42. Buses 40 and 42 are at substations 38 and 40, respectively, neither of which is flooded in any scenario; thus, lines 40-44 and 42-44 complete two conducting paths from the generation capacity at Bus 52 to the rest of the transmission network. Similarly, the MB deployed at the destination of Line 25-47 in each scenario and the one deployed at the origin of Line 47-51 in each scenario together indirectly link the generation capacity at Bus 25 to Bus 51. Bus 51 is at Substation 47, which is not flooded in any scenario; therefore, lines 25-47 and 47-51 provide one conducting path from the generation capacity at Bus 25—and thus also from the generation capacity at buses 10 and 22, through lines 10-25 and 10-22—to the rest of the transmission network.

VI. CONCLUSION

This article has presented a stochastic program that, in advance of a large-scale flood event, recommends the staging of mobile-substation resources as well as their anticipated operation in conjunction with permanent-substation restoration. Additionally, this article has propounded a parallel heuristic to efficiently solve instances of the stochastic program. OFAT experiments in the IEEE 24-Bus System have demonstrated the speed and solution quality of the heuristic, while a factorial experiment in a synthetic Houston grid has elucidated the relative influences of maximum total restoration labor system-wide per interval, maximum restoration labor at a substation per interval, and mobile-substation resource allowance on recovery of an inundated transmission network. Even when isolated from effects related to restoration of permanent substations, the effect of four mobile transformers and eight mobile breakers for a realistic set of flood scenarios in the synthetic Houston grid was found to be an average total-cost reduction of approximately $35MM (i.e., approximately 8% of a default optimal objective value).

REFERENCES

[1] *Hurricane Harvey Event Analysis Report*, North American Electric Reliability Corporation, Atlanta, GA, USA, Mar. 2018.

[2] *Substation Hardening for Electricity Resiliency*, North Carolina Utilities Commission, Duke Univ., Durham, NC, USA, 2019.

[3] (Aug. 2018). *Hardening the System After Historic Harvey*. Entergy Newsroom. [Online]. Available: https://www.entergynewsroom.com/news/hardening-system-after-historic-harvey/

[4] *Hurricane Harvey Event Recap Report*, Aon Benfield, London, U.K., Mar. 2018.

[5] *Final Hurricane Matthew Situation Report*, U.S. Dept. Energy, U.S. Nat. Capital, Washington, DC, USA, Oct. 2016.

[6] R. Kuckro. (Oct. 2018). *Soaked Substations Trip up Post-Hurricane Power Restoration*. Environment & Energy Publishing. [Online]. Available: https://www.eenews.net/articles/soaked-substations-trip-up-post-hurricane-power-restoration/

[7] *2017 National Electrical Safety Code*, IEEE Standard C2-2017, 2017.

[8] *R-MAG Medium Voltage Outdoor Dead Tank Vacuum Magnetic Circuit Breaker Instruction Manual*, ASEA Brown Boveri, Zürich, Switzerland, Feb. 2009.

[9] *IEEE Standard for Control Cabinets for Power Transformers*, IEEE Standard C57.148-2020, 2020.

[10] R. Daniels, D. Champagne, D. Alban, and M. Walcott, "Entergy's record flooding across our grid," in *Proc. 70th Annu. Conf. Protective Relay Engineers (CPRE)*, College Station, TX, USA, Apr. 2017, pp. 1–4.

[11] N. Abi-Samra and W. Henry, "Actions Before. and after a flood," *IEEE Power Energy Mag.*, vol. 9, no. 2, pp. 52–58, Mar. 2011.

[12] A. Fischbach. (Sep. 2017). *Hurricane Harvey Floods Entergy's Substations and Infrastructure. T&D World*. [Online]. Available: https://www.tdworld.com/electric-utility-operations/media-gallery/20970184/hurricane-harvey-floods-entergys-substations-and-infrastructure

[13] D. Holly. (Sep. 2017). *Louisiana Co-Op Helps Entergy With Harvey Recovery*. National Rural Electric Cooperative Association. [Online]. Available: https://www.electric.coop/washington-st-tammany-electric-entergy-substation

[14] S. Greenley, "Texas strong: Hurricane Harvey response and restoration," CenterPoint Energy, Houston, TX, USA, Tech. Rep. 1, Feb. 2018.

[15] *Benefits of Using Mobile Transformers and Mobile Substations for Rapidly Restoring Electrical Service*, U.S. Dept. Energy, U.S. Nat. Capital, Washington, DC, USA, Aug. 2006.

[16] AIEE Committee Report, "Working group report on mobile substations—Their use and the design of distribution substations to facilitate their use," *Trans. Amer. Inst. Electr. Eng.*, vol. 77, no. 3, pp. 193–200, Apr. 1958.

[17] J. Lopez-Roldan, C. Devriendt, J. Enns, R. Gijs, and P. Guillaume, "How to achieve a rapid deployment of mobile substations and to guarantee its integrity during transport," *IEEE Trans. Power Del.*, vol. 23, no. 1, pp. 196–202, Jan. 2008.

[18] (2018). *Mobile Circuit Switchers & Circuit Breakers (Product Page)*. Mobile Energy. [Online]. Available: http://mobileenergyinc.com/switchersandbreakers/
[19] D. Lubkeman and D. E. Julian, "Large scale storm outage management," in *Proc. IEEE Power Eng. Soc. Gen. Meeting*, Denver, CO, USA, Jun. 2004, pp. 16–22.
[20] *Tropical Storm Harvey Event Report (Update #9)*, U.S. Dept. Energy, U.S. Nat. Capital, Washington, DC, USA, Aug. 2017.
[21] Corporate Editorial Team. (Sep. 2017). *Entergy Texas Continues Harvey Restoration*. Entergy Newsroom. [Online]. Available: https://www.entergynewsroom.com/article/entergy-texas-continues-harvey-restoration/
[22] *Guidelines for Handling Water-Damaged Electrical Equipment*, National Electrical Manufacturers Association, 2005.
[23] *Evaluating Water-Damaged Electr. Equip.*, National Electrical Manufacturers Association, 2016.
[24] C. Yung and J. Bryan, "What to do after the storm: Maintenance and restoration planning for natural disaster recovery," *IEEE Ind. Appl. Mag.*, vol. 22, no. 5, pp. 12–19, Sep. 2016.
[25] *Spare Parts Programs for HV Equipment*, General Electric, Boston, MA, USA, Aug. 2020.
[26] *Considerations for a Power Transformer Emergency Spare Strategy for the Electric Utility Industry*, Electric Power Research Institute, Washington, DC, USA, Sep. 2014.
[27] A. M. Caunhye, X. Nie, and S. Pokharel, "Optimization models in emergency logistics: A literature review," *Socio-Econ. Planning Sci.*, vol. 46, no. 1, pp. 4–13, Mar. 2012.
[28] A. Arif, S. Ma, and Z. Wang, "Optimization of transmission system repair and restoration with crew routing," in *Proc. North Amer. Power Symp. (NAPS)*, Denver, CO, USA, Sep. 2016, pp. 1–6.
[29] P. Van Hentenryck, C. Coffrin, and R. Bent, "Vehicle routing for the last mile of power system restoration," in *Proc. 17th Power Syst. Comput. Conf.*, Stockholm, Sweden, Aug. 2011.
[30] C. Coffrin and P. Van Hentenryck, "Transmission system restoration: Co-optimization of repairs, load pickups, and generation dispatch," in *Proc. Power Syst. Comput. Conf.*, Wroclaw, Poland, Aug. 2014, pp. 1–8.
[31] A. Arab, A. Khodaei, S. K. Khator, and Z. Han, "Electric power grid restoration considering disaster economics," *IEEE Access*, vol. 4, pp. 639–649, 2016.
[32] Z. Qin, Y. Hou, S. Liu, J. Yan, and D. Li, "A branch-and-cut method for computing load restoration plan considering transmission network and discrete load increment," in *Proc. Power Syst. Comput. Conf.*, Wroclaw, Poland, Aug. 2014, pp. 1–7.
[33] Z. Song and H.-D. Chiang, "A rolling two-stage QGS-based method for transmission system restoration," in *Proc. IEEE Power Energy Soc. Gen. Meeting (PESGM)*, Denver, CO, USA, Jul. 2022, pp. 01–05.
[34] J. Yan and K. Xie, "Repair task scheduling of transmission systems considering conditional setup times," in *Proc. IEEE Power Energy Soc. Gen. Meeting (PESGM)*, Atlanta, GA, USA, Aug. 2019, pp. 1–5.
[35] X. Gao and Z. Chen, "Optimal restoration strategy to enhance the resilience of transmission system under windstorms," in *Proc. IEEE Texas Power Energy Conf. (TPEC)*, College Station, TX, USA, Feb. 2020, pp. 1–6.
[36] S. Liao, W. Yao, X. Han, J. Wen, and Y. Hou, "Two-stage optimization method for network reconfiguration and load recovery during power system restoration," in *Proc. IEEE Power Energy Soc. Gen. Meeting (PESGM)*, Denver, CO, USA, Jul. 2015, pp. 1–5.
[37] L. Sun, Z. Lin, Y. Xu, F. Wen, C. Zhang, and Y. Xue, "Optimal skeleton-network restoration considering generator start-up sequence and load pickup," *IEEE Trans. Smart Grid*, vol. 10, no. 3, pp. 3174–3185, May 2019.
[38] M. Zhao, P. R. Maloney, X. Ke, J. C. B. Ceballos, X. Fan, and M. A. Elizondo, "Power system recovery coordinated with (non-)black-start generators," in *Proc. IEEE PES Gen. Meeting (PESGM)*, Orlando, FL, USA, Jul. 2023, pp. 1–5.
[39] A. Arab, A. Khodaei, S. K. Khator, K. Ding, V. A. Emesih, and Z. Han, "Stochastic pre-hurricane restoration planning for electric power systems infrastructure," *IEEE Trans. Smart Grid*, vol. 6, no. 2, pp. 1046–1054, Mar. 2015.
[40] C. Coffrin, P. Van Hentenryck, and R. Bent, "Strategic stockpiling of power system supplies for disaster recovery," in *Proc. IEEE Power Energy Soc. Gen. Meeting (PESGM)*, Detroit, MI, USA, Jul. 2011, pp. 1–8.
[41] K. Lai, Y. Wang, D. Shi, M. S. Illindala, X. Zhang, and Z. Wang, "A resilient power system operation strategy considering transmission line attacks," *IEEE Access*, vol. 6, pp. 70633–70643, 2018.
[42] M. Movahednia, A. Kargarian, C. E. Ozdemir, and S. C. Hagen, "Power grid resilience enhancement via protecting electrical substations against flood hazards: A stochastic framework," *IEEE Trans. Ind. Informat.*, vol. 18, no. 3, pp. 2132–2143, Mar. 2022.
[43] S. Biswas, M. K. Singh, and V. A. Centeno, "Chance-constrained optimal distribution network partitioning to enhance power grid resilience," *IEEE Access*, vol. 9, pp. 42169–42181, 2021.
[44] S. Cai, Y. Xie, Q. Wu, M. Zhang, X. Jin, and Z. Xiang, "Distributionally robust microgrid formation approach for service restoration under random contingency," *IEEE Trans. Smart Grid*, vol. 12, no. 6, pp. 4926–4937, Nov. 2021.
[45] S. Lei, C. Chen, H. Zhou, and Y. Hou, "Routing and scheduling of mobile power sources for distribution system resilience enhancement," *IEEE Trans. Smart Grid*, vol. 10, no. 5, pp. 5650–5662, Sep. 2019.
[46] S. Lei, J. Wang, C. Chen, and Y. Hou, "Mobile emergency generator pre-positioning and real-time allocation for resilient response to natural disasters," *IEEE Trans. Smart Grid*, vol. 9, no. 3, pp. 2030–2041, May 2018.
[47] A. Arif, Z. Wang, C. Chen, and B. Chen, "A stochastic multi-commodity logistic model for disaster preparation in distribution systems," *IEEE Trans. Smart Grid*, vol. 11, no. 1, pp. 565–576, Jan. 2020.
[48] A. Arif, S. Ma, Z. Wang, J. Wang, S. M. Ryan, and C. Chen, "Optimizing service restoration in distribution systems with uncertain repair time and demand," *IEEE Trans. Power Syst.*, vol. 33, no. 6, pp. 6828–6838, Nov. 2018.
[49] B. Taheri, A. Safdarian, M. Moeini-Aghtaie, and M. Lehtonen, "Enhancing resilience level of power distribution systems using proactive operational actions," *IEEE Access*, vol. 7, pp. 137378–137389, 2019.
[50] S. Lei, C. Chen, Y. Li, and Y. Hou, "Resilient disaster recovery logistics of distribution systems: Co-optimize service restoration with repair crew and mobile power source dispatch," *IEEE Trans. Smart Grid*, vol. 10, no. 6, pp. 6187–6202, Nov. 2019.
[51] A. Arif, Z. Wang, J. Wang, and C. Chen, "Power distribution system outage management with co-optimization of repairs, reconfiguration, and DG dispatch," *IEEE Trans. Smart Grid*, vol. 9, no. 5, pp. 4109–4118, Sep. 2018.
[52] N. Rhodes and L. A. Roald, "Co-optimization of power line shutoff and restoration under high wildfire ignition risk," in *Proc. IEEE Belgrade PowerTech*, Belgrade, Serbia, Jun. 2023, pp. 1–7.
[53] C. Coffrin and P. Van Hentenryck, "A linear-programming approximation of AC power flows," *INFORMS J. Comput.*, vol. 26, no. 4, pp. 718–734, May 2014.
[54] M. Baran and F. F. Wu, "Optimal sizing of capacitors placed on a radial distribution system," *IEEE Trans. Power Del.*, vol. 4, no. 1, pp. 735–743, Jan. 1989.
[55] M. E. Baran and F. F. Wu, "Optimal capacitor placement on radial distribution systems," *IEEE Trans. Power Del.*, vol. 4, no. 1, pp. 725–734, Jan. 1989.
[56] M. E. Baran and F. F. Wu, "Network reconfiguration in distribution systems for loss reduction and load balancing," *IEEE Trans. Power Del.*, vol. 4, no. 2, pp. 1401–1407, Apr. 1989.
[57] J. Winkler, L. Dueñas-Osorio, R. Stein, and D. Subramanian, "Performance assessment of topologically diverse power systems subjected to hurricane events," *Rel. Eng. & Syst. Saf.*, vol. 95, no. 4, pp. 323–336, Apr. 2010.
[58] M. H. Amirioun, F. Aminifar, and H. Lesani, "Towards proactive scheduling of microgrids against extreme floods," *IEEE Trans. Smart Grid*, vol. 9, no. 4, pp. 3900–3902, Jul. 2018.
[59] Probability Methods Subcommittee, "IEEE reliability test system," *IEEE Trans. Power App. Syst.*, vol. PAS-98, no. 6, pp. 2047–2054, Nov. 1979.
[60] (2023). *Gurobi Optimizer Reference Manual*. Gurobi Optimization, LLC. [Online]. Available: https://www.gurobi.com
[61] Z. Zhang, H. Yang, X. Yin, J. Han, Y. Wang, and G. Chen, "A load-shedding model based on sensitivity analysis in on-line power system operation risk assessment," *Energies*, vol. 11, no. 4, p. 727, Mar. 2018.
[62] D. C. Montgomery, *Design and Analysis of Experiments*, 10th ed. Hoboken, NJ, USA: Wiley, Jun. 2020.

[63] A. B. Birchfield, T. Xu, K. M. Gegner, K. S. Shetye, and T. J. Overbye, "Grid structural characteristics as validation criteria for synthetic networks," *IEEE Trans. Power Syst.*, vol. 32, no. 4, pp. 3258–3265, Jul. 2017.
[64] *PSS E 33 Program Operation Manual (POM)*, Siemens PTI, Munich, Germany, 2020.
[65] K. Y. Kim, W.-Y. Wu, E. Kutanoglu, J. J. Hasenbein, and Z.-L. Yang, "Hurricane scenario generation for uncertainty modeling of coastal and inland flooding," *Frontiers Climate*, vol. 3, Mar. 2021, Art. no. 610680.

JOSHUA J. YIP (Member, IEEE) received the B.S. degree in electrical engineering and computer engineering from the University of Washington, Seattle, WA, USA, in 2015, and the M.S. and Ph.D. degrees from the Electrical and Computer Engineering Graduate Program, The University of Texas at Austin, Austin, TX, USA, in 2020 and 2023, respectively. His current research interest includes the application of mathematical optimization to the resilience and reliability of the electric grid.

VINICIUS C. CUNHA (Member, IEEE) received the M.Sc. and Ph.D. degrees in electrical engineering from the University of Campinas, Brazil, in 2017 and 2022, respectively. He was a Visiting Ph.D. Student with The University of Texas at Austin, in 2020. Since 2022, he has been a Researcher with Energy Research and Analytics (ERA). His research interests include analysis of distribution systems, smart meters, and grid-forming inverters.

BRENT G. AUSTGEN (Graduate Student Member, IEEE) received the B.S. degree in mathematics from the Rose-Hulman Institute of Technology, in 2014, and the M.S. degree from the Operations Research and Industrial Engineering program, The University of Texas at Austin, in 2020, where he is currently pursuing the Ph.D. degree with the Operations Research and Industrial Engineering Program. His current research pertains to the use of mathematical optimization for improving power system resilience to climate change and extreme weather events.

SURYA SANTOSO (Fellow, IEEE) is a Professor of electrical and computer engineering with The University of Texas at Austin, and holds the Engineering Foundation Centennial Teaching Fellowship in electrical engineering. His research interests lie in the broad area of transmission, distribution, microgrid systems, grid resilience, power quality, and data analytics. He is the sole author of *Fundamentals of Electric Power Quality* and the coauthor of *Electrical Power Systems Quality* (3rd edition). Additionally, he is an Editor of the *Handbook of Electric Power Calculations* (4th edition) and *Standard Handbook for Electrical Engineers* (17th edition). He is the Past Chair of the IEEE PES Transmission and Distribution Committee.

ERHAN KUTANOGLU received the Ph.D. degree in industrial engineering from Lehigh University. He is an Associate Professor of operations research and industrial engineering with the Cockrell School of Engineering, The University of Texas at Austin. His current research interests focus on integrated humanitarian logistics, particularly hurricane and other extreme weather event mitigation, preparedness, and recovery decision making and optimization. His goal is to combine predictive science-based models with prescriptive stochastic optimization models to develop an end-to-end understanding of uncertainty and optimized decision making in humanitarian logistics and disaster resilience, particularly for critical infrastructure, such as healthcare and power grid. His other interests span manufacturing and service logistics optimization, including network design, inventory management, transportation, and production planning and scheduling. He is an Active Member of INFORMS and IISE. He was a recipient of the NSF CAREER Award and the IBM Faculty Award.

JOHN J. HASENBEIN is a Professor with the Graduate Program in OR/IE, Department of Mechanical Engineering, The University of Texas at Austin. He has been supported by NSF via an International Research Fellowship and a CAREER Award, among other grants. He has provided research consulting to organizations, such as AMD, International Sematech, Samsung, Ayata, Zilliant, ConocoPhillips, SK-Telecom, STP Nuclear Operating Company, and the Department of Homeland Security. His research specialties include stochastic modeling, decision making under uncertainty, risk analysis, queueing theory, and statistical modeling.